

M-AM-Min1 LOCALIZATION OF CALMODULIN AND CHARACTERIZATION OF CALMODULIN BINDING PROTEINS IN THE VERTEBRATE ROD OUTER SEGMENT. D. Roof and M. Applebury, Purdue University, W. Lafayette, IN 47907 and J. Kirsch, University of Bonn, Bonn, West Germany.

Calmodulin is present in the vertebrate rod outer segment (ROS) in very low amounts. Immuno-fluorescent localization suggests that calmodulin is restricted to a "ciliary stripe" region in ROS. Calmodulin, actin, and microtubule antibodies co-localize to a stripe which originates at the inner segment/outer segment junction and extends more than a third of the way to the ROS tip. Cattle and toad ROS preparations were tested for potential calmodulin binding proteins by calmodulin overlay on blots. Calcium-dependent calmodulin binding proteins in cattle ROS are identified as 240K, 165K, 76K, 70K, 65K, 62K, and 53K polypeptides. In toad ROS similar polypeptides of 240K, 165K, 70K, and 53K are observed as well as several other polypeptides. The 240K polypeptide in cattle and toad has been shown to be antigenically related to the 240K subunit of fodrin, a spectrin-like actin- and calmodulin-binding protein from brain. A polyclonal antibody to mouse brain fodrin that cross reacts with toad brain fodrin also binds to both cattle and toad ROS 240K on blots. In toads fodrin co-localizes with calmodulin as shown by indirect immunofluorescence. The fodrin-like 240K polypeptide is distinct from "rim protein" (ROS 1.2) since the two can be resolved by 5% SDS-PAGE and neither the fodrin antibody nor calmodulin bind to "rim protein." None of the remaining calmodulin binding proteins correspond to the known light-regulated ROS proteins: rhodopsin, 48K, G-protein, or cGMP phosphodiesterase. These studies suggest that one role for calcium regulation in the ROS might be to mediate cytoskeletal interactions.

M-AM-Min2 KINETIC MEASUREMENT OF cGMP CHANGES IN INTACT PHOTORECEPTORS. Richard H. Cote and M. Deric Bownds, Laboratory of Molecular Biology, University of Wisconsin, Madison, Wisconsin.

For cGMP to act as an intermediate between light-induced activation of rhodopsin in the disc membrane and sodium permeability changes in the plasma membrane, light-induced changes in cGMP must be as rapid as the conductance change. Using a photoreceptor preparation of frog rod outer segments with the ellipsoid portion of the inner segment still attached, sub-second changes in cGMP levels upon illumination have been correlated with electrophysiological changes monitored by the suction electrode method. Within 200 msec after onset of bright, continuous illumination a significant decrease in cGMP concentration is observed in Percoll-Ringers' solution containing 1 mM Ca^{++} . Subsecond kinetics of cGMP changes were obtained by means of a rapid quench apparatus that mixed acid with rod suspensions and provided a time resolution of 50 msec. Subsecond changes in cGMP concentration are also observed by rapid freezing of photoreceptor suspensions. Rapid changes in cGMP levels are also observed at lower light intensities. Rods in 10^{-9} M Ca^{++} medium exhibit more rapid kinetics, the initial change in cGMP levels being complete in 50 msec.

This resolves the issue of whether changes in cGMP concentration in the rod under physiological conditions occur rapidly enough to potentially be involved in controlling the decrease in sodium conductance.

M-AM-Min3 STRUCTURE AND FUNCTION OF TRANSDUCIN. Yee-Kin Ho and Bernard K.-K. Fung, Department of Radiation Biology and Biophysics, University of Rochester Medical Center, Rochester, New York 14642

Phototransduction in vertebrate retinas involves a light-activated enzyme cascade that leads to a rapid reduction of cGMP level in the rod outer segments. Transducin, a GTP-binding regulatory protein consisting of two subunits (T_α , Mr. ~39,000 and T_β , Mr. ~36,000, ~6,000), mediates the signal coupling between rhodopsin and a cGMP phosphodiesterase in retinal rods. The T_α subunit is the activator of the phosphodiesterase and the T_β subunit serves to link T_α with rhodopsin. Proteolysis has been used to characterize the molecular structure of transducin subunits. TPCK-trypsin, *Staph. aureus* protease and submaxillary protease were used to generate an overlapping set of proteolytic fragments from T_α . Analysis of the amino terminal residue of each fragment has enabled us to establish a unique topological alignment of the proteolytic products. The locations of sulfhydryl groups on this linear peptide map and their functions were characterized by chemical modification. Our results showed that the carboxyl-terminal peptide of T_α and a specific sulfhydryl group located between 50 to 110 amino acid residues from the amino-terminal were essential for the activation of transducin by photolyzed rhodopsin. The GTP binding site was located in the middle portion of the T_α polypeptide chain. Upon the binding of Gpp(NH)p to this site, T_α undergoes a large conformational transition which has been identified by the changes in sulfhydryl reactivity and proteolytic fragmentation pattern.

M-AM-Min4 A MONOCLONAL ANTIBODY TO THE GUANINE NUCLEOTIDE BINDING PROTEIN BLOCKS THE LIGHT-ACTIVATED CYCLIC GMP PATHWAY IN FROG ROD PHOTORECEPTORS. Heidi E. Hamm, Department of Visual Science, School of Optometry, Indiana University, Bloomington, IN 47405.

A monoclonal antibody that blocks the light-activated cyclic GMP pathway in frog photoreceptor outer segments has been obtained. The antibody (4A) inhibits guanine nucleotide binding to the G-protein, the intermediate that links rhodopsin excitation to cyclic GMP phosphodiesterase (PDE), inhibiting light-induced PDE activity as a consequence. Antibody inhibition of the light-activated cGMP pathway is complete at a stoichiometry of approximately one antibody per G-protein in the mixture, indicating high specificity of the inhibition. Inhibition is more pronounced than that caused by PDE inhibitors isobutylmethylxanthine or Ro 20-1724. Antibody 4A has the further effect of inhibiting the phosphorylation of two low molecular weight proteins, Components I and II, whose phosphorylation normally can be stimulated by raising cGMP levels. The inhibition is not overridden by adding cGMP, suggesting that the G-protein influences these phosphorylations by a pathway distinct from its action on cGMP concentration. Antibody 4A may prove useful as a probe of the relevance of the cyclic GMP pathway to visual transduction in living photoreceptors.

M-AM-Min5 STRUCTURAL AND FUNCTIONAL CHARACTERIZATION OF PARVALBUMIN-LIKE PROTEINS IN FROG ROD OUTER SEGMENTS. Nancy W. Downer and Linda M. Siemankowski, Department of Biochemistry, University of Arizona, Tucson, AZ 85721

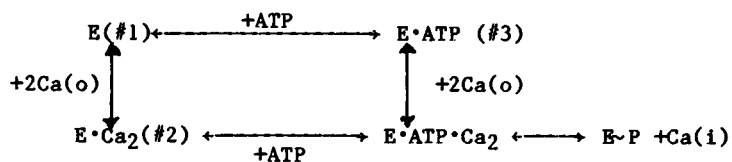
Since Ca^{++} serves as an intracellular messenger in rod photoreceptors, there are likely to be Ca^{++} -binding proteins in the rod cell that function in the reception of Ca^{++} signals and the feedback control of Ca^{++} movements within the cell. Using an antiserum raised against parvalbumin, a Ca^{++} -binding protein purified from frog muscle, we have shown by western blotting that purified rod outer segments contain a family of proteins related to parvalbumin. The smallest (~ 12 kdal) is similar in size to muscle parvalbumin, but at least two other larger proteins are recognized on blots. None of the proteins appears to be present in copy numbers greater than 1 per 1000 rhodopsin molecules. These parvalbumin-like proteins are characterized with respect to their Ca^{++} -binding, membrane association, light-dependent phosphorylation, and relationship to known light-regulated proteins in rod outer segments. Antibody purified from the anti-parvalbumin serum is used to investigate the role of the parvalbumin-like proteins in the Ca^{++} and cGMP regulatory pathways of retinal photoreceptors.

M-AM-A1 A COMPARISON OF CANINE CARDIAC SARCOLEMMAL AND SARCOPLASMIC RETICULUM PHOSPHOPROTEINS. Charles F. Louis and Janet Turnquist, Department of Veterinary Biology, University of Minnesota, St. Paul, Minnesota 55108.

The calmodulin + Ca, and cAMP-dependent protein kinase (cAMP-PK)-mediated phosphorylations of canine cardiac sarcolemma (SL) and sarcoplasmic reticulum (SR) vesicles have been compared. The objective has been to determine whether the 23,000-dalton, major SL protein kinase substrate, represents contamination of SL by SR-derived phospholamban (the major SR protein kinase substrate). Alamethecin, which unmasks latent SL activities (Manalan and Jones, J. Biol. Chem. 257, 10052-10062, 1982), stimulates the endogenous cAMP-PK-dependent phosphorylation of both SL and SR approx. 4-fold. In contrast, this polypeptide ionophore inhibits the calmodulin-mediated phosphorylations of both membranes. These results with alamethecin do not necessarily indicate that the SL phosphoprotein is due to SR-derived phospholamban. Similarities in the calmodulin-mediated phosphorylation of the SL and SR phosphoproteins include Mg^{2+} , Na^+ , Ca^{2+} and calmodulin sensitivities, as well as the characteristic inhibition of the disassociation of both 23,000-dalton phosphoproteins by $MgCl_2$. In contrast, a number of differences between these phosphoproteins was indicated in their sensitivities to detergents (Triton X-100 and sodium dodecyl sulfate) and calmodulin antagonists (R 24571 and Trifluoperazine). While these results confirm a number of similarities in the 23,000-dalton SL and SR phosphoproteins, they do not support the conclusion that the 23,000-dalton SL phosphoprotein represents SR-derived phospholamban contamination. (Supported by NIH, HL-25880).

M-AM-A2 INITIAL RATES OF CALCIUM TRANSLOCATION BY SARCOPLASMIC RETICULUM. Frederic Mandel. Dept. of Pharmacology and Cell Biophysics, Univ. of Cincinnati, College of Medicine, Cincinnati, Ohio 45267

The translocation of calcium from the outside (o) to the inside (i) of sarcoplasmic reticulum (SR) vesicles is associated with the $Ca^{2+}Mg^{2+}$ -ATPase (E) present in the SR membrane. The initial steps of the reaction mechanism may be represented by the following scheme:



With the recent advent of rapid mixing quench-flow techniques, the translocation of calcium and the formation of the acid stable phosphorylated intermediate of the $Ca^{2+}Mg^{2+}$ -ATPase (E-P) have been studied in the millisecond time range. Previous studies have either

started with "EGTA preincubated" SR (#1) and the reaction initiated by the simultaneous addition of calcium and ATP or with "calcium preincubated" SR and the reaction initiated by ATP. In the present study, we examined the kinetics of calcium translocation and E-P formation under the more physiological conditions of "ATP preincubated" SR. The initial rates (0-50 msec) of calcium translocation as a function of ATP concentration were determined. Our results also indicate that the binding of calcium and ATP to the $Ca^{2+}Mg^{2+}$ -ATPase are not independent but cooperative. (Supported by NIH HL 26049 and by a Research Career Development Award, HL 00789.)

M-AM-A3 LUMINESCENCE STUDIES OF TERBIUM BOUND TO THE Ca -ATPASE OF SARCOPLASMIC RETICULUM Terrence L. Scott, Dept. of Muscle Research, Boston Biomedical Research Institute, Boston, MA 01890.

Analysis of the kinetics of Tb^{3+} inhibition of enzyme activity and of Ca^{2+} protection of same indicate that initial lanthanide ion binding to the ATPase occurs at the high affinity Ca^{2+} sites, in agreement with a recent report (Highsmith and Head, JBC, 258, 6858, 1983).

The luminescence properties of Tb^{3+} bound to these sites on the ATPase have been examined via direct excitation of the lanthanide with a pulsed laser source. Measurements of the differences in Tb^{3+} luminescence lifetimes in H_2O and D_2O have been used to probe the molecular environment of the binding sites. The results indicate that there are ~ 2 water molecules in the first coordination sphere of Tb^{3+} bound at the high affinity sites.

Luminescence energy transfer measurements between the lanthanide binding site and suitable acceptors in the nucleotide binding domain have been done. Results suggest that the lanthanide site is at a considerable distance ($R > 35 \text{ \AA}$) from the catalytic domain. The implications of the results for localization of the ion sites of the ATPase within the Ca^{2+} pump complex will be discussed. Supported by NIH grant GM 32247.

M-AM-A4 PRODUCTION AND CHARACTERIZATION OF MONOCLONAL ANTIBODIES DIRECTED AGAINST THE CYTOPLASMIC FACE OF THE SARCOPLASMIC RETICULUM. Kevin P. Campbell, Craig Bomgaars, Gerald H. Denney and Alan Sharp, Dept. of Physiology and Biophysics, The University of Iowa, Iowa City, IA 52242

Monoclonal antibodies directed against sarcoplasmic reticulum proteins were prepared by cell fusion of mouse myeloma cells (NS-1) with spleen cells from mice immunized with purified sarcoplasmic reticulum vesicles from rabbit skeletal muscle. Selection of hybridoma cell lines that secreted monoclonal antibodies directed against the cytoplasmic face of the sarcoplasmic reticulum was based upon the ability of hybridoma culture supernatants to react with intact sarcoplasmic reticulum vesicles in an ELISA screening assay. Selected colonies were cloned and then grown in serum-free medium (HB102). Monoclonal antibodies (mabs) were purified to homogeneity directly from the HB102 culture medium. When analyzed by the immunoblot technique, five mabs recognized the 105,000 Da Ca^{2+} + Mg^{2+} ATPase, two recognized the 53,000 Da glycoprotein and two recognized a 20,000 Da protein of the sarcoplasmic reticulum. The mabs to the ATPase have been characterized with respect to their ability to recognize the major tryptic fragments of the ATPase and their effects on Ca^{2+} transport. The mabs to the 53,000 Da glycoprotein have been shown to react with both skeletal and cardiac glycoprotein, with the 49,000 Da carbohydrate-free form of the glycoprotein and with the high molecular weight glycoprotein from both skeletal (160,000 Da) and cardiac (130,000 Da) sarcoplasmic reticulum. The monoclonal antibodies are currently being used to localize the ATPase and glycoprotein in adult rabbit skeletal muscle using immunoelectron microscopy with Gold-Colloidal conjugated goat anti-mouse IgG. (Supported by NIH grant (NS 18814) and March of Dimes).

M-AM-A5 CALCIUM RELEASE INDUCED BY HEAVY METALS IS SIMILAR TO PHYSIOLOGICAL CALCIUM RELEASE FROM SARCOPLASMIC RETICULUM. Jonathan J. Abramson, Guy Salama*. Portland State University, Dept. of Physics, P.O. Box 751, Portland, OR 97207, and *Dept. of Physiology, University of Pittsburgh, Pittsburgh, PA 15261.

We have previously shown that low concentrations of various heavy metals cause a rapid increase in the Ca^{2+} permeability of SR vesicles (Abramson et al., Proc. Natl. Acad. Sci. USA, 1983,80:1526). We now show that heavy metals and other sulfhydryl reagents interact with a protein found in the heavy sarcoplasmic reticulum (HSR) fraction, but not found in the light sarcoplasmic reticulum (LSR) fraction. Addition of micromolar concentrations of Ag^+ induces 100% of the Ca^{2+} to be released at rates that are greater than our mixing times ($>50\text{nmol Ca}^{2+}/\text{mg}/\text{sec}$). Increases in the Ca^{2+} permeability are inhibited by various inhibitors of Ca^{2+} induced Ca^{2+} release. Tetracaine ($<1\text{mM}$), procaine ($<10\text{mM}$) and ruthenium red ($\sim 5\mu\text{M}$) are all shown to inhibit Ag^+ stimulated Ca^{2+} release in SR vesicles. These concentrations of the local anaesthetics procaine and tetracaine have been shown by others to inhibit caffeine stimulated and Ca^{2+} stimulated Ca^{2+} release and contraction in skinned fibre experiments. Using an ATP regenerative system, we also show that ruthenium red reversibly inhibits the Ca^{2+} permeability increase stimulated by the addition of Ag^+ .

The rate and extent of heavy metal stimulated Ca^{2+} release along with the fact that release is specific for HSR vesicles and is inhibited by various inhibitors of physiological Ca^{2+} release indicates that heavy metals are triggering release by binding to the physiological Ca^{2+} release protein from sarcoplasmic reticulum.

Supported by PSU Research and Publications, Oregon Affiliate of AHA, PHS Grant NS 18590, AHA Grant 82 1231 and Western Pennsylvania AHA.

M-AM-A6 DISTANCES BETWEEN BINDING SITES ON SR CaATPase by Stefan R. Highsmith, Department of Biochemistry, University of the Pacific, San Francisco, CA 94115

Nd^{3+} binding to sarcoplasmic reticulum (SR) was detected by inhibition of ATPase activity and directly by a fluorimetric assay. The results indicated that Ca^{2+} -activated ATPase activity is inhibited when about 10 nmol of Nd^{3+} per mg of SR bind specifically at the high-affinity Ca^{2+} binding sites. The association constant for Nd^{3+} binding was estimated to be $1 \times 10^9 \text{ M}^{-1}$.

Experiments were also done with SR labeled in the ATP binding site with fluorescein 5' -iso-thiocyanate (FITC). There was negligible fluorescence energy transfer (FET) from FITC to Nd^{3+} in the high-affinity Ca^{2+} binding sites. The distance between the FITC in the ATP site and Nd^{3+} in the high-affinity Ca^{2+} sites was estimated to be $\geq 3.3\text{nm}$.

At Nd^{3+} concentrations near $5 \times 10^{-6} \text{ M}$, binding occurred in sites that were 1.0 to 1.2 nm away from the FITC in the ATP site as determined by FET. Both Ca^{2+} and Mg^{2+} competed with Nd^{3+} for binding to these sites. For solutions containing 0.50 M KCl, pH 7 at 25°C , the following apparent association constants were obtained: $K_{\text{Nd}} = 3.3 \times 10^5 \text{ M}^{-1}$, $K_{\text{Ca}} = 84 \text{ M}^{-1}$ and $K_{\text{Mg}} = 35 \text{ M}^{-1}$. In all cases the apparent Hill coefficient was 1.3 ± 0.1 .

Tb^{3+} has been shown to bind similarly to the high affinity Ca^{2+} binding sites and the low affinity cation site(s). (1983, J. Biol. Chem. 258, 6858) Preliminary measurements of FET from Tb^{3+} to Nd^{3+} , with both bound to the high affinity Ca^{2+} binding sites, suggest the sites are less than 1 nm apart. Thus it appears that the high affinity Ca^{2+} sites are close to one another and far from the ATP site.

(NIH Grants AM25177 & AM00509)

M-AM-A7 REVERSAL KINETICS OF THE Ca^{2+} - Mg^{2+} -ATPase PUMP OF SKELETAL SARCOPLASMIC RETICULUM

Duncan H. Haynes, Dept. of Pharmacology, Univ. of Miami School of Medicine, Miami, Fl.

The kinetics of the Ca^{2+} pump reversal were studied as a means of determining the rate constant for the back reactions. Active uptake was initiated by adding 0.2 mM MgATP to sarcoplasmic reticulum preincubated with 0.67 μM Ca^{2+} (0.35 mM Ca^{2+} + 0.5 mM EGTA), 0.6 M sucrose, 100 mM KCl, 0.1 mM MgCl to 20 mM Tris, 10 mM HEPES, pH 7.0, 30°C. Active uptake and release were measured by chlorotetracycline fluorescence ($1 \times 10^6 \text{M}$) which is proportional to $[\text{Ca}^{2+}]_i$. After maximal Ca^{2+} uptake is observed, pump reversal was initiated by the following agents: EGTA, ADP and Pi. The insert gives the release conditions and the rates of loss calculated as $(1/t_{1/2}) \times \text{Fraction lost}$. The three agents increased the reversal rate to a value comparable to that of active uptake. ADP concentrations giving half-maximal effect ranged from 0.4 to 1.0 mM. The rates of reversal showed a biphasic dependence on K^+ concentration with an optimum of 50 mM. Supported by GM 23990.

| [EGTA] | [Ca^{2+}] | [ADP] | [Pi] | Rate of loss |
|--------|----------------------|-------|------|-------------------|
| mM | μM | mM | mM | sec ⁻¹ |
| 0 | 0.67 | 0.0 | 0.0 | 0.03 |
| 0 | 0.67 | 0.0 | 0.1 | 0.10 |
| 0 | 0.67 | 2.0 | 1.0 | 0.13 |
| 0 | 0.67 | 2.0 | 0.1 | 0.12 |
| 0 | 0.67 | 2.0 | 1.0 | 0.32 |
| 3 | 0.029 | 0.0 | 0.1 | 0.23 |
| 3 | 0.029 | 0.0 | 1.0 | 0.43 |
| 3 | 0.029 | 2.0 | 0.1 | 0.46 |
| 3 | 0.029 | 2.0 | 1.0 | 0.50 |

M-AM-A8 CALCIUM-CALMODULIN-DEPENDENT REGULATION OF CARDIAC SARCOPLASMIC RETICULUM FUNCTION. B.A. Davis, A. Schwartz, and E.G. Kranias. Department of Pharmacology and Cell Biophysics, University of Cincinnati College of Medicine, Cincinnati, Ohio 45267

Cardiac sarcoplasmic reticulum (SR) contains an endogenous calcium-calmodulin (CAM) dependent protein kinase (CAM-PK) and a substrate, phospholamban. This kinase is half maximally activated (EC_{50}) by 3.8 μM Ca^{2+} and is absolutely dependent on exogenous CAM ($\text{EC}_{50} = 49 \text{ nM}$). To determine the effect of this phosphorylation, SR vesicles were preincubated under conditions for optimal phosphorylation while control vesicles were preincubated under identical conditions but in the absence of ATP. Both control and phosphorylated SR were centrifuged and subsequently assayed for Ca^{2+} transport in the presence of 2.5 mM Tris-oxalate. The amount of CAM remaining in both control and phosphorylated SR, as determined by radioimmunoassay, was not sufficient to result in activation of the CAM-PK during transport. Phosphorylation of SR by CAM-PK resulted in significant increase (2-4 fold, $n=9$, $p<0.003$) in the rate of Ca^{2+} transport at low Ca^{2+} concentrations ($<3 \mu\text{M}$), while Ca^{2+} transport at higher Ca^{2+} concentrations ($>3 \mu\text{M}$) was minimally affected. Hill coefficients (n) derived from Hill plots of transport data showed no difference between control and phosphorylated SR ($n=2.2$) indicating no change in cooperativity upon phosphorylation. However, the EC_{50} for Ca^{2+} activation of Ca^{2+} transport was significantly decreased by 30% ($n=9$, $p<0.003$), indicating an increase in the apparent affinity for Ca^{2+} upon phosphorylation. Preliminary results on the action of CAM-dependent phosphorylation indicate a lack of effect on the Ca^{2+} -ATPase activity when assayed under these same conditions. (Supported by NIH grants HL26057, HL22619, HL00775, HL07382, and by an A.J. Ryan Fellowship Award to B.A.D.)

M-AM-A9 PROPERTIES OF A PHOSPHOPROTEIN PHOSPHATASE ACTIVITY ASSOCIATED WITH CARDIAC SARCOPLASMIC RETICULUM. Evangelia G. Kranias. Department of Pharmacology and Cell Biophysics, University of Cincinnati College of Medicine, Cincinnati, Ohio 45267

The calcium pump in cardiac sarcoplasmic reticulum (SR) appears to be regulated through phosphorylation of phospholamban, a 22,000 dalton polymeric proteolipid. Phospholamban is phosphorylated by cAMP-dependent and Ca^{2+} -calmodulin-dependent protein kinases, on sites which appear to be distinct from each other, and both types of phosphorylation are associated with stimulation of Ca^{2+} transport. We report here the presence of an endogenous phosphoprotein phosphatase activity in cardiac SR, which catalyzes the reverse reactions, that is, dephosphorylation of phospholamban. To determine some of the characteristics of the phosphatase, the time course of SR dephosphorylation was followed in the presence of various reactants, using SR vesicles prephosphorylated by either cAMP-dependent or Ca^{2+} -calmodulin-dependent protein kinases. The rate of dephosphorylation was maximally stimulated by Mn^{2+} while Mg^{2+} /ATP had less of a stimulatory effect. The presence of EGTA or Ca^{2+} and calmodulin had no significant effects compared to control, and fluoride inhibited the phosphoprotein phosphatase activity. The effects of the various reactants were similar for dephosphorylation of either the cAMP-dependent or Ca^{2+} -calmodulin-dependent sites. These findings indicate the presence of a phosphoprotein phosphatase in cardiac SR which can dephosphorylate both sites on phospholamban, and this is probably the enzyme participating in regulation of cardiac SR function *in vivo*. (Supported by NIH grants HL26057 and HL00775)

M-AM-A10 REGULATION OF Ca^{2+} TRANSPORT BY CYCLIC 3':5'-AMP-DEPENDENT AND CALCIUM-CALMODULIN-DEPENDENT PHOSPHORYLATION OF CARDIAC SARCOPLASMIC RETICULUM. Evangelia G. Kranias. Dept. of Pharmacology and Cell Biophysics, Univ. of Cincinnati College of Medicine, Cincinnati, Ohio 45267

Canine cardiac sarcoplasmic reticulum (SR) is phosphorylated by cyclic AMP-dependent and by Ca^{2+} -calmodulin-dependent protein kinases on a 22,000 M_r protein called phospholamban. Both types of phosphorylation have been shown to stimulate the initial rates of Ca^{2+} transport. To establish the interrelationship of the cAMP-dependent and Ca^{2+} -calmodulin-dependent phosphorylation on Ca^{2+} transport, cardiac SR vesicles were preincubated under optimum conditions for: a) cAMP-dependent phosphorylation, b) Ca^{2+} -calmodulin-dependent phosphorylation, and c) both. Control vesicles were treated under identical conditions but, in the absence of ATP, to avoid phosphorylation. Control and phosphorylated SR vesicles were subsequently centrifuged and then assayed for Ca^{2+} transport in the presence of 2.5 mM Tris-oxalate. Our results indicate that cAMP-dependent and Ca^{2+} -calmodulin-dependent phosphorylation can each stimulate calcium transport in an independent manner, and when both are operating, they appear to have an additive effect. Regulation of Ca^{2+} transport was associated with a statistically significant increase in the apparent affinity (EC_{50}) for calcium by each type of phosphorylation. The degree of stimulation of the calcium affinity was relatively proportional to the degree of phospholamban phosphorylation. These findings suggest the presence of a dual control system which may operate in independent and combined manners for regulating cardiac sarcoplasmic reticulum function. (Supported by NIH grants HL26057 and HL00775.)

M-AM-B1 TROPONIN-TROPOMYOSIN COMPLEX CONFERS Ca^{++} CONTROL TO MYOSIN BEAD MOVEMENT IN VITRO. Ronald Vale*, Andrew Szent-Gyorgyi† and Michael Sheetz (Intr. by Dennis Koppel). Department of Physiology, University of Connecticut Health Center, Farmington, CT 06032.

In skeletal muscle the Ca^{++} -dependence of contraction results from a conformation change of the troponin-tropomyosin complex upon binding Ca^{++} . In the algal cell, *Nitella*, there is no known troponin-tropomyosin complex bound to the cell's actin cables. We have indeed found that the movement of skeletal myosin coated beads on *Nitella* actin is Ca^{++} -independent over a range of Ca^{++} concentrations from 10^{-9} to 10^{-4}M . If rabbit skeletal muscle troponin-tropomyosin is added to *Nitella* then the movement of skeletal myosin coated beads is Ca^{++} dependent. The concentration of Ca^{++} required for half maximal activation of bead movement in the presence of troponin-tropomyosin is $10\text{ }\mu\text{M}$ which compares favorably with the concentration required to half maximally activate ATPase by troponin-tropomyosin coated actin. Addition of either troponin or tropomyosin alone is without effect on motility. Incubation of the troponin-tropomyosin with myosin saturated beads is also without effect. Only when both are present on the *Nitella* does bead movement become Ca^{++} dependent. This provides the first demonstration of the reconstitution of Ca^{++} dependent motility with an actin-based regulation system. Because the troponin-tropomyosin requires extensive controls with the actin filaments, the results suggest that *Nitella* actin is free to bind added proteins. Further, it is possible to use the *Nitella* based motility assay to study the effects of actin-binding proteins on motility.

*Department of Neurobiology, Stanford University Medical School, Stanford, CA 94305.

†Department of Biology, Brandeis University, Waltham, MA 02254.

M-AM-B2 MYOSIN THREADS. P.H. Cooke, E.M. Bartels, G.F. Elliott and K. Jennison, The Open University, Oxford Research Unit, Berkeley Road, Boars Hill, Oxford, OX1 5HR, U.K..

KCl-filled microelectrodes record Donnan potentials from A- and I-bands of glycerinated rabbit psoas and of (chemically) skinned rat semitendinosus muscle; from this potential the electric charge on the contractile proteins can be calculated (Collins and Edwards, *Am. J. Physiol.*, 1971, 221:1130; Elliott and Bartels, *Biophys. J.*, 1982, 38:195). Direct light-microscope observation locates the microelectrode tip. In rigor the A-band potential is significantly greater than the I-band potential; in relaxation the two are equal. (Bartels and Elliott, *J. Physiol.* 1981, 317:85P; 1982, 327:72P; 1983, 343:32P). So in rigor, not in relaxation, there is a charge difference between the A- and I-bands of muscle, and since it does not depend on filament overlap the extra myosin charge occurs independently of cross-linking of the two sets of filaments. To clarify the charging process, we prepare threads of myosin, ~ 0.4mm diam., protein concentration 120-150 mg/ml (comparable to muscle A-bands). Charge measurements give ~ 100 electrons/molecule in 50 mM KCl rigor solution, and ~ 65 e/mol in 20 mM KCl rigor solution; these values are similar to those from rigor muscle. E/m sections show that in 20 mM KCl the myosin filaments are uniform in diameter and length, and pack quasi-regularly into bundles of A-band dimensions. We have recorded meridional (14.3nm) and equatorial (38nm) X-ray reflections. The threads swell rapidly (25% in diam) when the salt concentration is increased or nucleotides are added, and transparency changes accompany the swelling.

M-AM-B3 CROSS-BRIDGE KINETICS OF RABBIT SKELETAL MUSCLE FIBERS WHEN THE LATTICE SPACE IS ALTERED BY DEXTRAN T-500 AND IONIC STRENGTH CHANGES. M. Kawai, M.I. Schulman, and T. Cornacchia. Department of Anatomy and Cell Biology, Columbia University, New York, N.Y. 10032

Chemically skinned single fibers were prepared from rabbit psoas (fast) and semitendinosus (slow) muscles, and subjected to maximal activation at $\text{pCa } 5$ and $1\text{-}5\text{mM MgATP}$. The experiment was carried out in the presence of an impermeable macromolecule Dextran T-500, which is known to shrink the lattice space (Godt & Maughn, 1977). In order to determine the effect of the macromolecule on the cross-bridge kinetics, complex stiffness and tension of fibers were observed. The ionic strength was adjusted by NaCl/KCl, and the lattice space was estimated by the diameter of the fiber. At a constant ionic strength, the tension increased to reach a maximum at 4-7% Dextran, while complex stiffness and associated rate constants were not altered, except for magnitude parameters which were scaled with tension. At higher concentrations, the tension was slow to develop and complex stiffness was severely affected, appearing as if the viscosity greatly increased so as to decrease the rate constants and to diminish oscillatory work. The increase in tension with 4-7% Dextran was 10% at a low ionic strength (150mM), whereas it was 300% at a high ionic strength (350mM). Since increase in ionic strength generally increases the lattice space and decreases Ca-activated tension without affecting the rate constants, it can be concluded that the ionic strength effect is partially reversed by Dextran. These results generally confirm that there is an optimal lattice space for cross-bridge cycling and force production, and that the ability to perform work rapidly diminishes when the lattice is compressed below this level.

M-AM-B4 STRUCTURAL AND VOLUME CHANGES IN ISOLATED CARDIAC MUSCLE CELLS IN DETERGENT AND HIGH IONIC STRENGTH MEDIA. Kenneth P. Roos and Allan J. Brady. Dept. Physiol. UCLA LA CA 90024

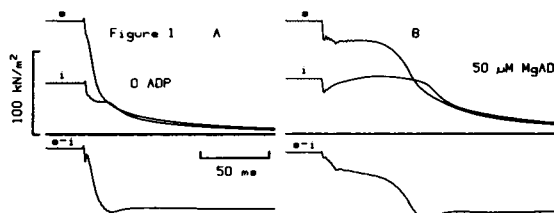
Sarcomere lengths (SL), cell lengths (CL) and widths (CW), and general structural uniformity were obtained from photomicrographs and direct CCD computer imaging of single isolated cardiac muscle cells (myocytes) which were enzymatically digested from whole rat hearts (Roos & Brady, *Biophys. J.* 40:233-244, 1982). Untethered, resting myocytes were examined first in a standard Tyrode's medium containing 0.25 mM Ca^{++} and 20 mg/ml albumin. After a rapid solution change to a K^+ , EGTA-based relaxing media ($\text{pCa} = 9$), cell volume increased by 8% ($P < 0.005$) due exclusively to CW increase. The addition of 0.5% Triton X-100 detergent to the relaxing medium induced an additional 8% ($P < 0.005$) volume increase due to further width expansion. There were no changes in SL ($1.89 \pm 0.10 \mu\text{m}$, $n = 17$) or CL. In high ionic strength solution (0.42M KCl-pyrophosphate), most cells shortened in seconds, to an average $1.47 \pm 0.11 \mu\text{m}$ SL without a CW change, thus eliciting a 15% cell volume decrease ($P < 0.025$). Prior to shortening, most cells demonstrated a reversal of the striation pattern contrast and a doubling of the periodicity indicating the likely dissociation of the myosin filaments. Further exposure to a higher ionic strength 0.6M KCl solution elicited an additional 17% cell volume decrease ($P < 0.005$) due to both CW and SL/CL decreases. The periodicity was $1.19 \pm 0.19 \mu\text{m}$ in these cell ghosts. Variation in measured SL and striation pattern uniformity remained consistent at less than 10% in each media except KI, which was somewhat higher. These data suggest that cardiac muscle cells swell as a result of an expansion of the myofilament lattice. However, the presence of a longitudinal constraining element in the intact cell is suggested by the shortening of the cell at reduced cell volume in high ionic strength media. (Supported by USPHS HL29671 and HL30828)

M-AM-B5 THE INHIBITION OF MUSCLE CONTRACTION BY LIGANDS THAT BIND AT THE ATP SITE ON MYOSIN E. Pate and R. Cooke, Department of Mathematics, W.S.U., Pullman WA 99163, and Dept of Biochemistry and Biophysics, and CVRI, University of California, San Francisco CA 94143

The maximum velocity of glycerinated psoas muscle is inhibited by the presence of PPi , AMPPNP and ADP . These ligands all act as pure competitive inhibitors with K_i 's of 5 mM (AMPPNP), 3 mM (PPi) and approximately 0.3 mM (ADP). These results were analyzed in terms of a seven state model of myosin cross-bridge kinetics. The known binding constants of the ligands to actomyosin or to muscle fibers were used to define the free energies of the actin-myosin-ligand states. These ligands all bind tightly to actomyosin and analysis of the model showed that they should be stronger inhibitors than is observed. Previous work by others has shown that binding of these ligands to rigor muscle fibers causes an apparent increase in the length of the fibers. Such an increase could result if the axial position of the actomyosin-ligand state is shifted a few nanometers with respect to the actomyosin state. When such a shift was incorporated into the above model, the observed inhibition of velocity by the ligands could be explained. The ligands are weak inhibitors because at the end of the powerstroke, where ATP binds to the cross-bridge, the free energy of the ligand states has risen above that of the actomyosin state, promoting the dissociation of the ligand. This model was also consistent with the rates observed in solution for ligand association with and dissociation from actomyosin. This work was supported by grants from the USPHS HL16683, AM30868, AM00479 and from the NSF PCM8208292 and from the Research and Arts Committee of W. S. U.

M-AM-B6 ADP SLOWS CROSS-BRIDGE DETACHMENT RATE INDUCED BY PHOTOLYSIS OF CAGED ATP IN RABBIT PSOAS MUSCLE FIBERS. J.A.Dantzig*, M.G.Hibberd*, Y.E.Goldman* & D.R.Trentham*. Departments of Physiology* and of Biochemistry and Biophysics*, University of Pennsylvania, Philadelphia, PA 19104

When caged ATP was photolyzed to liberate ATP within skinned muscle fibers in rigor, the relaxation was associated with cross-bridge reattachment and force generation even in the absence of Ca^{2+} (*Nature* 300, 701-705; 1982). Extraction of the pure detachment rate required additional analysis. If the stress imposed by a length change is retained only as long as a cross-bridge remains continuously attached, tension traces, starting at different rigor tensions, would converge with the time course of detachment of the original rigor links. Rigor tension in consecutive trials was altered by a 0.2-0.8% stretch or release applied 1 s before the laser pulse. Algebraic differences between pairs of traces decayed with a half-time of ~8 ms at 500 μM MgATP (Fig. 1A). Pre-incubation of the fibers in ADP slowed convergence of tension records (Fig. 1B). At 50-500 μM MgADP and >500 μM MgATP, the convergence half-time (~60 ms) did not correlate with [ADP] or [ATP]. Assuming that Ca^{2+} does not influence the dissociation of ADP from A.M.ADP, these results suggest that dissociation of ADP may partially control the active cross-bridge cycle. Supported by NIH grants HL15835 and AM00745.



M-AM-B7 CONSTITUTIVE EQUATIONS OF SKELETAL MUSCLE BASED ON CROSS-BRIDGE MECHANISM. Aydin Tozeren, Intr. by Murray Eden, BEIB, DRS, NIH, Bethesda, MD 20205.

Statistical mechanics of cross bridge action is considered in order to develop constitutive equations that express fiber tension as a function of degree of activation and time history of speed of contraction. The kinetic equation of A.F. Huxley (Prog. Biophys. Mol. Biol. 7:255, 1957) is generalized to apply to the partially activated state. The rate parameters of attachment and detachment, and cross-bridge compliance are assumed to be step functions of extension, x , with a finite number of discontinuities. This assumption enables integration of the kinetic equation and its moments with respect to x analytically resulting in equations where x has been eliminated. When the constants in the rate parameters and the force function are chosen such that Hill's force-velocity relation and features of the transient kinetic and tension data can be fitted, the resulting cross bridge mechanism is quite similar to the one proposed by Podolsky and coworkers (Proc. Natl. Acad. Sci. USA, 64:504, 1969). Because the derived constitutive equations simplify mathematical analysis, they enable the evaluation of the influence of various cross-bridge parameters on the mechanical behavior of muscle fibers. For example (i) Instantaneous elastic response (T_0-T_1) and the magnitude of rapid recovery (T_2-T_1) after a step length change can be explained well when the rate of attachment is assumed high for positive x . In that case T_2 corresponds to the force generated by cross-bridges in the region of negative x . (ii) Kinetic transients occur as a result of the jumps that exist in the distribution of attached cross bridges during the isometric state. Because of the hyperbolic nature of the kinetic equation, these jumps propagate in the $-x$ direction causing rapid changes in the speed of contraction.

M-AM-B8 FUNCTION OF CREATINE KINASE LOCALIZATION IN MUSCLE CONTRACTION. Stephen J. Koons and Roger Cooke. CVRI and Dept. of Biochem./Biophysics, Univ. of Calif., San Francisco, CA 94143.

A small fraction of cytoplasmic creatine kinase (CK) is tightly bound to the contractile apparatus of skeletal muscle at the M-line. Together with reports that CK may bind to myosin, this observation suggested the hypothesis that the localized CK may supply ATP for contraction more effectively than soluble CK. The maximum velocity of contraction of glycerinated rabbit psoas fibers is proportional to the ATP concentration at low ATP levels, allowing us to measure the ability of both bound and soluble CK to regenerate ATP for acto-myosin. We therefore measured the velocities of fibers in lightly loaded isotonic contractions ($P=0.1P_0$) in 100 μ M ATP, 20 mM phosphocreatine (PCr), and in varying amounts of CK. In the absence of PCr, the velocity was only 0.02 length/s. Addition of 20 mM PCr increased the velocity to 0.11 length/s because of the presence of bound CK. This tightly bound CK, retained by the glycerinated fibers following storage and brief washing, was measured with a luciferase-luciferin assay system. When CK activity in the fiber was doubled by adding CK to the solution bathing the fiber, the velocity of contraction doubled. A linear relationship between velocity and CK activity was maintained to CK concentrations 5 times that of bound. If the intrinsic CK had been more effective at supplying ATP, we would have expected a greater velocity of contraction in the absence of added CK or a smaller increment in velocity upon addition of soluble CK. Because the fiber velocities respond equally to intrinsic and extrinsic CK, we conclude that the tightly bound fraction does not regenerate ATP for contraction more effectively than soluble CK. Supported by USPHS fellowship HL-06707 to SK, and grants HL-15683, AM-30868 and AM-00479 to RC.

M-AM-B9 X-RAY EVIDENCE FOR TWO STRUCTURAL STATES OF THE ACTOMYOSIN CROSSBRIDGE IN MUSCLE FIBERS. Takashi Matsuda and Richard J. Podolsky, (Intr. by Jay Miller) Lab. of Physical Biology, NIADDK, National Institutes of Health, Bethesda, MD 20205.

Actomyosin crossbridges form in relaxed skinned rabbit muscle fibers at low ionic strength (Brenner et al., PNAS, 1982, 79, 7288). In the present study we examined the structure of these crossbridges by small angle X-ray diffraction. At sarcomere length 2.3 μ m, the myosin layer lines and the intensity distribution along the 59 Å actin layer line of the relaxed fiber at low ionic strength ($\mu=20$ mM) were almost the same as those at normal ionic strength ($\mu=120$ mM). However, the 215 Å meridional reflection decreased in intensity in low μ and in rigor. At sarcomere length 4.0 μ m, the patterns in normal μ and low μ were almost same, which indicates that low μ does not have an "ordering effect" that could compensate for changes associated with cross-bridge formation. These results show that the structure of the low μ crossbridge is significantly different from that of the rigor crossbridge. This observation provides evidence for the existence of two different crossbridge structures: one that preserves the myosin based features of the diffraction pattern (low μ relaxed) and another that reduces the intensity of these features. The latter structure is associated with strongly-bound crossbridges (rigor, Ca-activated). The former structure is also found in the case of AMPPNP crossbridges (Tregear et al., in Crossbridge Mechanism in Muscle Contraction, (Sugi & Pollack, eds.) 1979, 407) and thus might be a general property of weakly-bound crossbridges.

M-AM-B10 TIME-RESOLVED X-RAY DIFFRACTION MEASUREMENTS OF THE ACTIVATION MECHANISM IN STRIATED MUSCLE. H.E. Huxley, M. Kress and A.R. Faruqi. MRC Laboratory of Molecular Biology, Hills Road, Cambridge, England. (Intr. by A.G. Szent-Györgyi)

Using synchrotron radiation from the storage ring DORIS, we have studied the behaviour of the actin pattern in frog sartorius muscles following stimulation. Earlier work had shown a characteristic increase in intensity on the second actin layer line at a radial spacing around 0.021\AA^{-1} , which could be interpreted in terms of a movement of tropomyosin towards the centre of the long pitch grooves in the actin helical structure (the steric blocking mechanism). The present work confirms the existence of this substantial intensity increase, specifically associated with the active state, and shows that it occurs earlier after the stimulus than any of the other changes in the X-ray diagram that we have studied. At 5°C , the average half-time for the change was 17 msec (48 experiments). Under similar conditions, the changes in the equatorial pattern (showing crossbridge attachment) have a half-time of about 25-30 msec, while half maximum tension is reached in about 45 msec. In semitendinosus muscles stretched beyond overlap, the intensity increase on the second layer line is still observed, and can have a similar magnitude to the change at normal overlap. These results indicate that in relaxed muscle under physiological conditions, the initial attachment of crossbridges is blocked by the troponin-tropomyosin system, and that when this inhibition is removed following stimulation, attachment takes place to an initial state which does not develop tension until a further rate process has occurred. The results also indicate that tropomyosin movement takes place independently of myosin attachment.

M-AM-B11 LIGHT DIFFRACTION PATTERN OF SKELETAL MUSCLE EXPLAINED WITH THE EWALD FORMALISM. F. Zite-Ferenczy*, K.D. Häberle*, W. Wilke*, and R. Rudel, Abt. Allgemeine Physiologie and Abt. Experimentelle Physik Universität D-7900 Ulm, FRG.

Light diffraction by skeletal muscle is influenced by volume effects. The use of the Bragg formalism for its description (J. Physiol. 290:317, 1979) has been criticized as too idealistic for a system with lattice planes as badly defined as they are in muscle. We now describe the diffraction pattern using Ewald's formalism in the reciprocal space (Math. Biochim. Anal. chapt. 13, pp. 113, 1965). We assume the diffracting elements to be bundles of myofibrils ("columns", diam. 5 to 15 μm) delineated from their neighbors by the fact that their lattice planes are of identical angle η with respect to a plane normal to the fiber axis. The lattice planes within a column are assumed to be of constant spacing L_s . Between adjacent columns, η can vary by up to $\pm 10^{\circ}$, while L_s varies by only $\pm 3\%$. For the majority of columns η is small. With this model we can explain the geometry of the layer lines, in particular its substructure (number and shape of the spots). At normal beam incidence and a given L_s there is an optimal angle η (approximately the Bragg-angle) for highest light intensity in a spot. The decrease of light intensity with increasing deviation from the optimum can be calculated. The considerations are applicable for any angle of beam incidence with respect to the fiber axis. The Ewald formalism allows better understanding of the diffraction pattern than models applied to muscle so far. It also illuminates the limitations intrinsic in frog muscle for the determination of L_s using light diffraction.

M-AM-B12 THREE-DIMENSIONAL RECONSTRUCTION OF NATIVE TARANTULA MUSCLE THICK FILAMENTS. R. Padrón*, R.A. Crowther and R. Craig**, MRC Laboratory of Molecular Biology, Hills Rd., Cambridge CB2 2QH, UK. Present address: *IVIC, Centro de Biofísica y Bioquímica, Apdo. 1827, Caracas 1010A, VENEZUELA; **Anatomy Department, University of Massachusetts Medical School, Worcester, MA 01605, USA.

Thick filaments from leg muscle of tarantula, maintained under relaxing conditions (Mg.ATP & EGTA) were negatively stained and photographed with minimal electron dose. Particles were selected for 3D image reconstruction by general visual appearance and by the strength and symmetry of their optical diffraction patterns, which extend meridionally to the 6th order of 435A, but appear to show peaks to higher radial resolution. Phase differences across the meridian indicated 4-fold rotational symmetry, so that on a given layer-line Bessel function contributions of different orders start to overlap at fairly low resolution, and must be separated computationally by combining data from different views. Two independent reconstructions agree well and show more detail than previous reconstructions of thick filaments (*Limulus*: Stewart et al. (1981), J. Mol. Biol. 153, 781-790; *scallop*: Vibert & Craig (1983), J. Mol. Biol. 165, 303-320). The strongest feature is a set of long pitch right-handed helical ridges (pitch $4 \times 435\text{\AA}$). There are also ridges with an axial spacing of 145A lying in planes roughly normal to the filament axis and running circumferentially. We suggest that the latter may be formed by the stacking of an S1 head from one myosin molecule on an S1 head from an axially neighbouring molecule. Internal features in the map indicate an approximate local 2-fold axis relating the putative heads. This interpretation must be checked by further work, but it does suggest that sufficient detail is present to make it worthwhile to undertake biochemical experiments to observe structural changes in the filaments.

M-AM-C1 THRESHOLD CHANNELS IN THE SQUID GIANT AXON. Wm. F. Gilly and Clay M. Armstrong, Hopkins Marine Station of Stanford University, Pacific Grove, CA., 93950 and Dept. of Physiology, University of Pennsylvania, Philadelphia, PA., 19104.

We report here the discovery of a new kind of TTX-sensitive Na channel in giant axons of *Loligo pealei* studied under the standard experimental conditions used in our laboratory. Conventional axial wire voltage clamp methods were used, and axons were internally perfused with either TMA or Cs to eliminate K currents. A major distinguishing characteristic of the new channels is their slow closing kinetics. Thus, Na tail currents show 2 grossly different rates of decay. At 8°C the two time constants are 150–200 μ s vs. 1–2 ms. The slow component is particularly visible for depolarizations to the threshold region, which selectively activates the slowly closing channels. Analysis of tail currents under a variety of activating conditions leads to the following conclusions. The new channels: 1) open with fairly normal kinetics, but close very slowly; 2) are selectively activated at voltages negative to the range of activating normal channels; 3) constitute at most a few percent of the total Na permeability; and 4) inactivate more or less normally, by a mechanism sensitive to internally applied pronase. Though constituting only a small fraction of total Na permeability, these channels can carry enough current to drive membrane potential well beyond action potential threshold. Because they are selectively activated by small depolarizations, the new channels must dominate behavior of the axon at threshold. We therefore label them "threshold channels."

M-AM-C2 KINETIC PROPERTIES OF SINGLE SODIUM CHANNELS. Carol A. Vandenberg and Richard Horn, Department of Physiology, UCLA Medical School, Los Angeles, CA 90024

Outside-out excised patch and whole cell recordings of sodium channel currents were obtained from cells of the rat pituitary cell line GH₃ in the presence of internal CsF at 90°C. Single channel recordings revealed that individual channels open and close several times during a single depolarizing test pulse, especially to potentials more hyperpolarized than -30 mV. Using a 3 state "fate" model (Aldrich, Corey, Stevens, *Nature*, in press) we found that the probability of an open channel inactivating (instead of closing) increased with depolarization, as did the rate constant, β_1 , for inactivating from the open state. We estimated rate constants for a general model with 5 states (3 closed, 1 open, 1 closed-inactivated) using a maximum likelihood method (Horn, Lange, 1983, *Bio-phys. J.* 43:207). Inactivation could occur from any state in this model. β_1 increased with depolarization, varying in different patches e-fold/19 to 35 mV, in agreement with results obtained using N-bromoacetamide (Horn, Vandenberg, Lange, *Biophys. J.*, in press). The closing rate constant was also voltage dependent, increasing with hyperpolarization, but the rate constants for inactivating from closed states were relatively voltage-independent. Our analysis suggests that macroscopic inactivation derives its voltage dependence from both the activation process and β_1 . Rate constants obtained from the maximum likelihood method provided excellent estimates of the open time, closed time, and first-latency densities, the time course of averaged currents, and the distribution of number of channel openings per record. Alternative hypotheses were compared using the likelihood-ratio test. Most could be statistically eliminated at the 0.1% level (e.g., Hodgkin-Huxley and strictly-coupled models). Statistically acceptable models allowed inactivation to occur from the open state as well as at least one of the closed states.

M-AM-C3 ESTIMATE OF THE SQUID AXON SODIUM CHANNEL CONDUCTANCE WITH IMPROVED FREQUENCY RESOLUTION. R. A. Levis, F. Bezanilla and R. M. Torres. Dept. of Physiology, Rush Medical College, Chicago, IL 60612 and Dept. of Physiology, UCLA, Los Angeles, CA 90024.

The cut-open axon technique was modified to simplify the recording of fluctuations of a small population of channels. A clean segment of squid giant axon was pinned to a Sylgard-lined chamber and was cut open in artificial sea water. The axoplasm was mechanically removed and a fire polished pipette with an aperture between 35 and 50 μ m in diameter was pressed against the internal side of the membrane. Seal resistance varied between 10 and 50 megohms. The pipette was connected to a current-to-voltage converter with a 100 megohms feedback resistor followed by a high frequency booster. The potential of the patch was varied by changing the bath voltage. Sodium currents showing good voltage control could be recorded with a bandwidth up to 25 KHz. We used nonstationary noise analysis techniques to estimate the single sodium channel conductance at different membrane potentials and with varying amounts of divalent cations. When exposed to external solutions containing 10 mM Ca and 50 mM Mg, the apparent single channel conductance, γ , was generally 5–6 pS for wideband measurements in the range of -30 to 0 mV. When the same patches were exposed to an external solution with 6 mM Ca and no Mg, the apparent γ consistently increased, e.g. at -20 mV, γ was about 8 pS for bandwidths of 20–25 kHz. Decreased bandwidths reduced the apparent channel conductance. These results indicate that sodium channels in squid axon have extremely fast fluctuations that can result in underestimated values of γ . They are also consistent with macroscopic measurements of block of the squid Na channel by external Ca and Mg reported by Taylor et al. (*Biophys. J.* 16:27a, 1976). Supported by USPHS grant GM30376.

M-AM-C4 SQUID AXON SODIUM CHANNEL: GATING CURRENT WITHOUT RISING PHASE. Stimers, J.R., Bezanilla, F. & Taylor, R.E. Dept. Physiology, UCLA, Los Angeles, CA 90024 and Lab Biophysics, NINCDS, NIH, Bethesda, MD 20205.

Perfused squid axons were voltage-clamped and gating current (I_g) was recorded using the P/4 procedure. A single pulse from -70 to -80 mV in full Na⁺ sea water outside and an isosmotic solution inside, produces a capacity transient (I_c) that decays rapidly with an apparent single time constant (about 2 μ s). Minutes after replacing external Na⁺ with Tris, a slow component develops with an apparent time constant on the order of 20 μ s. The total area and the fast time constant are not changed. These changes in I_c are reversed when the inside is made hyposmotic with respect to the outside so that water flows out of the axon. In parallel with these changes in I_c we observe that I_g has a rising phase when I_c has two components. The time course of the rising phase of I_g is the same as the slow component of I_c . I_g with or without rising phase have the same charge versus voltage curve when measured in the same axon. Also, I_g decay and charge immobilization are not affected by the osmotic gradient. These results could be obtained by increasing the external osmolality with sucrose, Na⁺, or Tris or by decreasing the internal osmolality. We conclude that the rising phase of the sodium gating current can be attributed to a distributed series resistance arising from a restricted Frankenhaeuser-Hodgkin space. When external Na⁺ is replaced by Tris, the high mobility of Na⁺ allows it to exit the F-H space before Tris can enter, collapsing the space. The imposed osmotic gradient expands the space reducing its resistance, thereby improving the spatial homogeneity of the voltage clamp.

Research was supported by USPHS grant #GM30376 and NIH Fellowship to JRS.

M-AM-C5 ZN IONS SELECTIVELY SLOW NA ACTIVATION AND INACTIVATION DELAY. L. Goldman, G.A. Ebert and R. Chandler, Dept. of Physiol., School of Med., Univ. of Maryland, Baltimore, MD 21201.

Inactivation in *Myxicola* Na channels develops with a delay, indicating a precursor process (Goldman and Kenyon, *J. Gen. Physiol.* 80:83, 1982). This precursor process is kinetically very similar to Na activation. The potential dependency of its time constant is the same as that of Na activation, differing significantly from that of τ_c and τ_h . And, when resolvable, the time constant of the delay is identical to $\tau_m(V)$. We report here that external Zn slows the time to half maximum g_{Na} ($t_{1/2}$) and inactivation delay in a parallel way (about 1.6-fold for 5 mM Zn). 1 mM Zn had no effect. If the change in $t_{1/2}$ is attributed entirely to surface potential effects, τ_c should have slowed by 2-fold while only 10% was observed, consistent with computations on a simple sequential coupled model. In addition in Zn: (i) Peak I_{Na} following brief conditioning steps always increased over the unconditioned value. Without Zn, brief conditioning pulses produced either no change or a slight decrease. (ii) Without Zn the delay decays as a simple exponential. With Zn the delay develops as two exponentials plus a third process completed by the first 200 μ s of conditioning at -22 mV, as expected if three sequential processes precede inactivation. Na activation in *Myxicola* also develops as three processes, one very rapid, providing further correspondence between Na activation and inactivation delay. These additional effects are consistent with the suggestion of Gilly and Armstrong (*J. Gen. Physiol.* 79:935, 1982) that Zn stabilizes the occupancy of the resting state(s) and so weights more heavily transitions preceding channel opening. g_{Na} time course in Zn is accurately reconstructed with a five state sequential coupled model using the measured τ_h and the time constants fitted to the inactivation delay time course, providing clear evidence that at least some fraction of Na channels conduct before they can inactivate. Supported by USPHS Grant NS-07734.

M-AM-C6 EVIDENCE FOR A SURFACE CHARGE NEAR THE INNER MOUTH OF THE SODIUM PORE OF SQUID GIANT AXONS. C. Smith, M.D. Cahalan*, & T. Begenisich. Dept. of Physiology, Univ. of Rochester, Rochester, NY 14642 *and Dept. of Physiology & Biophysics, Univ. of California, Irvine, CA 92717

We have used a monovalent and a divalent guanidinium analog to probe the surface charge near the inner mouth of the sodium pore in squid giant axons using internal perfusion and voltage-clamp techniques. The block of steady-state sodium channel current produced by the monovalent cation n-propylguanidinium (npG) and the divalent cation 1,3 bis-guanidino-n-octane (bis G₂) was measured as a function of internal ionic strength. The concentration of internal sodium was constant at 50 mM; ionic strength changes were made using cesium. With bisG₂ the block at a membrane potential near +95 mV is an extremely steep function of internal ionic strength but at the same potential the block produced by npG is less steep. These results demonstrate the presence of a negative surface charge near the inner entrance to the sodium pore. The data are quantitatively described by a model that combines the saturable binding of the guanidinium analogs to the pore (which blocks current flow) and a surface charge which attracts the compounds. There are, then, two parameters in this model: the equilibrium dissociation constant, K_d , and the surface charge density. The model also includes the approximately linear relationship between K_d and internal sodium concentration we have previously described. The block produced by both the monovalent and divalent analogs is accounted for by a surface charge density of $-1e/300 \text{ \AA}^2$. This is a much higher density than the $-1e/1000 \text{ \AA}^2$ obtained from the influence of ionic strength on the voltage-dependent activation of these channels and the value of $-1e/700 \text{ \AA}^2$ obtained from the voltage-dependence of inactivation. These results appear to question the validity of a literal interpretation of the "ball and chain" model of sodium channel inactivation.

M-AM-C7 VOLTAGE ACTIVATED RESONANCE IN GATING CURRENT Fohlmeister, J.F.¹ and Adelman, W.J., Lab of Biophysics, NINCDS, NIH, at M.B.L., Woods Hole, MA and ¹Physiology Dept., Univ. of Minn., Minneapolis MN

The technique of "voltage-activated-resonance" in nerve membranes is being developed for the purpose of resolving gating (or asymmetry) currents into components corresponding to individual voltage-sensitive molecular transitions. The forcing functions are sinusoidal changes in the electric field generated by a voltage-clamp. The output is the asymmetry current component of the dielectric displacement current that is generated at the stimulus frequency, f . The basic model for the approach is that the two molecular conformations involved in each isolated transition have equal probability of occurrence for one and only one membrane potential. Oscillating the membrane potential about that potential will drive the conformation change provided the frequency of oscillation stands in a particular relationship with the rate constant, k , for that transition at the membrane potential of equal probability. Thus the information contained in a gating current record is spread out in the plane with coordinates of frequency and mean membrane potential. The signal strength is adequate because the isolated species of molecular transitions are driven rather than passively observed at a single membrane potential. Mathematical analysis of the model shows that the amplitude (at the potential of equal population probability) increases with f for $f < k$ and then levels to a plateau value for $f > k$. The phase declines with increasing frequency to a value of 17.7° at $f = k$. A number of transitions have been isolated in preliminary experiments and the dynamic characteristics agree qualitatively with the mathematical analysis.

M-AM-C8 OSCILLATION-FREE COMPENSATION FOR RESISTANCE IN SERIES WITH EXCITABLE MEMBRANES.

John W. Moore, Michael Hines, and Edward M. Harris. Department of Physiology, Duke University Medical Center, Durham, NC 27710.

Extracellular resistances in series (R_s) with excitable membranes give rise to significant voltage errors which distort the current records in voltage clamps (e.g., squid axon membranes).

Two methods for electrical measurement of such resistances were used and evaluated. The conventional voltage jump in response to a current step was accurate to $\pm 0.5 \Omega \text{ cm}^2$ but a measurement of sine wave admittance under voltage clamp conditions was better, having about a 5-fold improvement in resolution over the conventional method.

Conventional voltage clamp feedback to correct the $R_s I_m$ error signal leads to instability when approximately 2/3 of the error is corrected. Circuit analysis and simulations show that stability of a voltage clamp circuit can be achieved along with full compensation for R_s by any means which reduces the feedback of capacitive current relative to ionic currents.

We describe our method of choice for an oscillation-free voltage clamp of squid axons which uses an active electronic bridge circuit to subtract membrane capacitive current (and leakage), allowing full R_s compensation for the voltage error due to ionic currents; but there is no R_s compensation during the time of significant capacitive current flow.

Marked changes in the kinetics and amplitude of ionic currents were observed for several typical potential patterns when full compensation for series resistance was introduced.

M-AM-C9 INTRACELLULAR NH_4^+ AND H^+ IONS ANTAGONIZE BLOCK OF SODIUM CHANNELS BY SAXITOXIN AND TETRODOTOXIN. G.S. Oxford, Paul Forscher*, and D.J. Adams. Department of Physiology, University of N.C., Chapel Hill, NC and the Marine Biological Laboratory, Woods Hole, MA.

The block of sodium channels by saxitoxin (STX) and tetrodotoxin (TTX) was examined in voltage-clamped squid giant axons internally perfused with NH_4^+ ions or with solutions of low pH. In control axons perfused with 300mM NH_4 the magnitude of outward currents through Na channels is nearly equal to that recorded with 120mM Na. In contrast when many of the channels were blocked by external STX or TTX, outward NH_4 currents were as much as 2X larger than outward Na currents. Hydrazinium currents were also larger than I_{Na} in the presence of toxin. Na currents at 0 mV are reduced by 50% at internal pH 5.5. Recovery of I_{Na} upon return to internal pH 7.3 is monotonic. The total block of Na currents by both low internal pH and external toxin treatment is less than the sum of blocks seen with either agent alone. In the presence of toxin a pH change from 5.6 to 7.3 results in a biphasic recovery of current characterized by a transient increase in both inward and outward I_{Na} . In the absence of toxin the block of Na channels by internal protons could be substantially relieved by increasing the external buffer strength (HEPES) from 5 to 25mM.

These results indicate significant interactions between blocking molecules which approach sodium channels from opposite sides. It is specifically suggested that (1) ammonium and hydrazinium can relieve toxin block of Na channels by donating protons to a binding site with the channel during ion passage, (2) protons introduced intracellularly compete for the same binding site as STX and TTX introduced extracellularly, and (3) protons can readily pass through open sodium channels.

(Supported by NSF grant BNS82-11580 to G.S.O.).

M-AM-D1 EFFECTS OF X-IRRADIATION OF SINGLE CRYSTALS OF RIBONUCLEASE A

S.K. Burley, G.A. Petsko & D. Ringe, Chemistry Department, Massachusetts Institute of Technology, Cambridge, MA 02139.

Radiation damage of biomolecules is an important yet poorly understood phenomenon. We have studied X-radiation damage of ribonuclease A by high-resolution X-ray crystallography. Structural changes induced by irradiation with 10Mrad were restricted to a few specific sites in the enzyme. All the disulphide bridges were opened and oxygen atoms appear to have been added to each sulphur atom. The four methionine residues appear to have been changed to methionine sulphones. The aromatic side chains also showed evidence of chemical modification. Despite the scission of the disulphide bridges, there was no major conformational change suggestive of general unfolding of the enzyme.

M-AM-D2 A THEORY OF GEL EXCLUSION CHROMATOGRAPHY. Charles P. Bean. General Electric Corporate Research and Development, Schenectady, NY 12301 and Rensselaer Polytechnic Institute, Troy, NY 12181.

Gel exclusion chromatograph is primarily used as a preparative technique for separating globular proteins. A column of porous beads is equilibrated with the medium in which the proteins are to be suspended. A mixture of suspended proteins is introduced, as a thin band, at the top of the column. After an amount of fluid, $V_e(MW)$ has eluted from the bottom of the column, the protein of a given molecular weight, MW , first appears in the elutant. The theoretical problem is to deduce $V_e(MW)$ as a function of the parameters of the column. These parameters include, V_o , the volume of the column external to the beads and the total internal porous volume, V_i , of the beads. This proposed theory assumes that the beads have uniform circular pores of a size that just exclude a molecular weight MW^* , and that conditions of quasi-equilibrium apply to the entry of uniform density spherical molecules into the pores. Further, it is assumed that the interaction of the molecules and the pores is a simple hard-core interaction. The resulting expression is $V_e(MW) = V_o + V_i \times (1 - (MW/MW^*)^{1/3})^2$, $MW \leq MW^*$. Experiments by Andrews (1965) are in striking agreement with the relationship shown above. MW^* is deduced to be $1.02 \pm .05 \times 10^6$ for Sephadex G-200 as employed by Andrews. Subsidiary calculations show that the results, for most of the range of molecular weights, to be quite insensitive to the assumptions of strictly uniform pores and of strictly spherical molecules. This equilibrium treatment is related to an earlier non-equilibrium proposal by Ackers (1964) - a proposal that appears to have been discarded, Ackers (1970). Andrews, P. 1965. *Biochem. J.* **96**, 595. Ackers, G. 1964. *Biochem. J.* **3**, 723. Ackers, G. 1970. *Adv. Protein Chem.* **24**, 343.

M-AM-D3 NOCODAZOLE-CALF BRAIN TUBULIN INTERACTION. Joseph D. Head*, John C. Link* and James C. Lee, Dept. of Biochemistry, St. Louis University School of Medicine, St. Louis, MO 63104.

Nocodazole is a synthetic drug which has been shown to have antimitotic and antitumoral activity. The primary target site of the drug is tubulin. However, the molecular mechanism(s) through which nocodazole exerts its effect is still unknown. A study was initiated to define the kinetic and equilibrium parameters which govern the interaction between nocodazole and calf brain tubulin in 10^{-2} M sodium phosphate, 10^{-4} M GTP and 12% (v/v) dimethylsulfoxide at pH 7.0. Stopped-flow spectroscopy was employed to monitor the rate of nocodazole binding under pseudo-first order conditions. The effects of temperature and nocodazole concentration were studied. The apparent rate constant is dependent on the concentration of nocodazole in a non-linear manner suggesting a mechanism of $T + N \rightleftharpoons TN \rightleftharpoons T^*N$, where T and N are tubulin and nocodazole, respectively. T and T* represent two conformational states of tubulin. Both the binding and conformational change are apparently entropy driven. The parameters derived from the rapid kinetic measurements are in good agreement with those determined by equilibrium binding studies.

M-AM-D4 ROLE OF ELECTROSTATIC INTERACTIONS IN ASSEMBLY OF *E. COLI* ASPARTATE TRANSCARBAMYLASE. M. Glackin-Sundell, M.P. McCarthy, N.M. Allewell, Department of Biology, Wesleyan University, Middletown, CT 06457; J.B. Matthew, Genex Corporation, Rockville, MD 20852.

Assembly of *E. coli* aspartate transcarbamylase in the reaction $6c + 6r \rightleftharpoons c_6r_6$ requires five types of protein-protein interactions (c1-c2, c1-c4, c1-r1, c1-r4 and r1-r2). We have used the Tanford-Kirkwood theory as modified by Gurd and coworkers (cf Biochemistry, 18, 1919 (1979)) to characterize the electrostatic effects associated with each interaction. Coordinates used were those made available to the Brookhaven Protein Data Bank by Honzatko et al (J. Mol. Biol. 160, 219 (1982)). The results provide information about the ionizable groups perturbed by each interaction and the contribution of electrostatic effects to the free energy of assembly. They also yield predictions about the variation in $\Delta\bar{v}_H^+$ (H^+ bound/contact formed) with pH and ionic strength which can be compared with experimental results. For example, the calculations indicate that the pK values of 6 c and 10 r chain residues shift by more than 0.1 pH unit as a result of formation of the c1-r1 interface at $I=0.1M$. Calculated values of $\Delta\bar{v}_H^+$ over the pH range 6-10 parallel values derived by potentiometry for the overall assembly reaction (McCarthy and Allewell, in press). The contribution of electrostatic interactions at this interface to the free energy of assembly varies from -12 kcal/m at pH 6 to +1.2 kcal/m at pH 10. Electrostatic interactions also stabilize the r1-r2 interface, but destabilize the c1-c4 interface between the two catalytic subunits. This result is of particular interest since binding of the allosteric effector PALA increases the distance between catalytic subunits.

Supported by NIH Grant AM-17335.

M-AM-D5 REVERSIBLE AND IRREVERSIBLE ELECTROSTATIC MODIFICATION OF AMINO GROUPS; ANION AFFINITY LABELING AND MODELS FOR ELECTROSTATIC INTERACTIONS IN PROTEIN CHEMISTRY. Scott Saunders, Stephenie Paine and Bo Hedlund, University of Minnesota, Minneapolis, MN 55455

The glyoxylate anion ($CHOCOO^-$) can be considered bifunctional. It has properties similar to those of a small anion (e.g. acetate). It also forms a reversible Schiff base with amino groups. Both properties will influence the interactions between the ion and proteins. Comparison of the binding properties of glyoxylate ion with an ion incapable of forming the Schiff base allows for partial separation of the two effects. The terminal α -amino groups of hemoglobin form Schiff bases with glyoxylate and also act as reporter groups for the presence of negative charge. Comparison of oxygen binding curves obtained with glyoxylate and a conventional ion show an enhancement of the anion allosteric effect of about 4 kcal/mole Hb tetramer due to Schiff base formation. Proteins existing in higher concentrations of glyoxylate ion take on a reversible bound shield of negative charge by virtue of Schiff base formation at lysine residues. The distribution can be considered "smeared" and is determined by electrostatic factors. This system can be utilized to study proteins under conditions where, in the absence of glyoxylate, aggregation occurs or solubility is limiting. This type of reversible modification of protein amino groups is conceptually related to reductive carboxymethylation. The latter is accomplished by the combined use of glyoxylate and cyanoborohydride which leads to irreversible incorporation of negative charge. The distribution of added carboxyl groups to protein amino groups is usually non-specific and can be considered "smeared" in a macroscopic sense. Supported by NIH Grant AM 28124.

M-AM-D6 SPECTROSCOPIC, ELECTROCHEMICAL, AND REACTIVITY STUDIES OF TYPE 2 COPPER-DEPLETED LACCASE. *R. Max Wynn, David B. Knaff, and Robert A. Holwerda, Department of Chemistry, Texas Tech University Lubbock, TX 79409.

Fluorescence, circular dichroism, and spectroelectrochemical studies of type 2 copper-depleted (T2D) *Rhus vernicifera* laccase have been performed to determine the influence of type 2 Cu removal on the polypeptide structure and physical properties of the type 1 and type 3 copper sites. The midpoint potentials (E^0) of the type 1 Cu in T2D_r (reduced type 3 center) and native laccases, determined with hydroxyethylferrocene (HEF) as mediator, are essentially identical (420 and 429 mV, respectively). Comparisons of the 300-700 nm CD spectra of native, T2D_r and T2D_{ox} (oxidized type 3 center) laccases reveal no detectable structural change at the type 1 copper center associated with removal of the type 2 Cu atom and only small effects of the oxidation state of the type 3 center on the environment of the type 1 site. Fluorescence measurements on Japanese-lacquer-tree (*Rhus vernicifera*) laccase and the fungal (*Polyporus versicolor*) enzyme show fluorescence emission near 420nm and phosphorescence emission in the 440-465 nm region. The fluorescence and phosphorescence excitation spectra for both laccases show maxima in the 310-330 nm range, a spectral region which corresponds to the absorbance maxima for the oxidized type 3 binuclear Cu centers of the two enzymes. Additional evidence links the newly discovered emissions with the type 3 Cu centers of the two laccases.

In addition, stopped-flow kinetic studies of electron transfer from HEF and seven hydroquinones to *Rhus vernicifera* T2D_r type 1 Cu (II) were performed to verify the importance of type 2 copper in the binding of polyphenolic substrates.

Supported by the Robert A. Welch Foundation Grant (D-710) to D.B.K.

M-AM-D7 LIGAND BINDING EFFECTS ON THE HYDROGEN EXCHANGE RATES OF LYSOZYME by Roger B. Gregory, Ann Dinh, and Andreas Rosenberg, University of Minnesota, Minneapolis, MN 55455

The active site cleft of lysozyme can accommodate six units of the N-acetylglucosamine oligosaccharide substrate within sites designated A,B,C,D,E and F to give a productive complex which subsequently undergoes glycoside cleavage between sites D and E. Lysozyme also forms non-productive complexes with oligosaccharides in which one or more of the A, B and C sites are occupied. N-acetylglucosamine trimer (Tri-NAG) forms such a non-productive complex with the A, B and C sites. The influence of Tri-NAG binding to lysozyme on the conformational dynamics of the enzyme has been studied by measuring the hydrogen exchange rates of the free enzyme and 1:1 enzyme - Tri-NAG complex. Exchange rates of the faster exchanging protons are only decreased by a factor of 2-3 while those of the 15-20 slowest exchanging protons are decreased by a factor of 10-50 by the binding of Tri-NAG. In lysozyme, many of the slowest exchanging protons are located within the dynamically stable β -sheet and buried α -helix segments to which the active site carboxylates of Asp 52 and Glu 35 are attached. The results indicate that the perturbation of conformational dynamics brought about by ligand binding at the A, B and C sites is propagated throughout the active site cleft and is experienced by those stable secondary structural segments that are closely associated with the active site carboxylates at the glycoside cleavage site. Evidently, part of the free energy realized by binding ligand at sites A, B and C is retained by the protein, rather than being dissipated as heat and is transferred to the glycoside cleavage site to facilitate subsequent difficult steps along the reaction pathway (free energy complementarity, Lumry and Biltonen, 1969). Supported by NSF PCM 8003744.

M-AM-D8 POSITIVE COOPERATIVITY IN BINDING CARBON MONOXIDE TO HEMOCYANIN

Brough Richey, Heinz Decker and Stanley J. Gill, Department of Chemistry, University of Colorado, Boulder, CO 80309

The binding of oxygen and carbon monoxide to hemocyanins from the crab *Scylla serrata* and the lobster *Homarus americanus* was studied by thin layer optical absorption and front face fluorescence techniques. In the case of *S. serrata*, the binding of carbon monoxide and oxygen to the dissociated monomeric form is completely noncooperative. As expected, the binding of oxygen to the native oligomeric form is found to be strongly cooperative. Surprisingly, the binding of carbon monoxide to this form is found to be weakly but definitely cooperative. In the case of *H. americanus*, the binding of oxygen and carbon monoxide to the monomeric form is also found to be completely noncooperative, and the binding of oxygen to the oligomeric form is cooperative. The lower affinity of carbon monoxide to this hemocyanin makes the direct detection of positive cooperativity difficult. However, experiments involving the binding of both oxygen and carbon monoxide in the presence of each other require an analysis which leads to the conclusion that carbon monoxide binding is slightly cooperative. For both these hemocyanins a three state allosteric model is found to be necessary in order to completely describe the binding of both ligands under a variety of ligand partial pressures. This work was supported by NIH Grant 22325.

M-AM-D9 KINETIC STUDIES OF THE ASPARTYL PROTEASES WITH VARIATION IN THE P3 RESIDUE OF CHROMOPHORIC PEPTIDE SUBSTRATES Ben M. Dunn, John Kay, Melba Jimenez, Martin J. Valler, Jaya K. Rao, and Benne F. Parten Dept. of Biochemistry & Molecular Biology University of Florida College of Medicine Gainesville, Florida 32610

We have prepared by solid phase peptide synthesis a new series of peptide substrates of the general structure Lys-Pro-X-Glu-Phe-(NO₂)Phe-Arg-Leu. Porcine pepsin and other related enzymes cleave these peptides between the Phe and (NO₂)Phe residues generating a shift in the ultraviolet spectra of the nitrophenylalanyl chromophore sufficient to permit the collection of kinetic data. Product analyses have been carried out by isolation of cleaved fragments and have confirmed the position of attack as indicated. We have obtained K_m and k_{cat} values for our series of six analogs for pepsin and at least four other aspartyl proteases. In addition we have determined the pH and temperature dependence of hydrolysis for the optimal substrate. Recent crystallographic results have pointed out the extended nature of the hydrophobic active site cleft of this group of enzymes (Bott, et al., (1982) *Biochem. J.* 21, 6956-62; James, et al., (1982) *Proc. Natl. Acad. Sci.*, 79, 6137-41). We have observed considerable variation in the kinetic parameters within this series of substrates for reaction with the individual enzymes. This could arise from the effect of binding interactions at the P3 subsite upon the reactive (enzyme or substrate) configuration around the P1 - P1' peptide bond. We also observed large differences in these parameters from enzyme to enzyme within the Aspartyl Protease family. This must reflect subtle differences in the structure of the active sites of this group of related enzymes.

M-AM-D10 uncA Mutant F_1 -ATPases:Uncooperative Catalysis. Wise, J.G., Ferguson, A.M., Latchney, L.R. and Senior, A.E., Department of Biochemistry, University of Rochester, Rochester, NY 14642.

The α -subunit of the catalytic sector (F_1) of the H^+ -ATPase of *E. coli* is coded by the uncA gene. Three point mutations (uncA401, uncA447 and uncA453) result in formation of F_1 of normal size and subunit composition, but with defective catalysis. Normal (very low) rates of ATP hydrolysis were observed when substrate bound to only one catalytic site per uncA F_1 , suggesting that unpromoted catalysis was inherently similar to normal. The large enhancement of ATP hydrolysis rate (measured as P_i formation) observed with unc⁺ F_1 when more than one catalytic site was saturated by substrate (1900x) was not observed with the uncA F_1 -ATPases. Instead, only small enhancement was seen (1.4x, 5x, 11x). Relative ATPase activity versus ATP·Mg concentration curves suggested that only limited residual catalytic cooperativity was retained by the uncA F_1 -ATPases. Each uncA F_1 had a normal complement of adenine nucleotide binding sites (six per F_1) with lower than normal affinity for ATP·Mg and AMPPNP·Mg at the first catalytic site. Investigations of nucleotide specificity (unc⁺ F_1) in binding, catalysis and F_1 -bound aurovertin fluorescence enhancement experiments indicated that the defective intersubunit interaction described previously in these uncA F_1 -ATPases (Wise, J.G., Latchney, L.R., Senior A.E. (1981) J. Biol. Chem. 256 10383) occurs between a catalytic nucleotide site (β -subunit) and an aurovertin binding site (β -subunit) and is mediated by α -subunit. We therefore suggest that the uncA401, uncA447 and uncA453 mutations impair cooperative interactions between catalytic sites which are required for normal catalytic function. Supported by NIH grant GM25349.

M-AM-E1 LOCATION OF THE MODIFIER SITE OF THE HUMAN ERYTHROCYTE ANION EXCHANGE SYSTEM. Philip A. Knauf and Nancy A. Mann, Department of Radiation Biology and Biophysics, University of Rochester Medical Center, Rochester, NY 14642.

Chloride and other halides at high concentrations inhibit red cell anion exchange by binding to a modifier site, which is distinct from the anion transport site (Dalmark, J. Gen. Physiol. (1976) 67: 223-234). To determine the side of the membrane at which this modifier site is located, we varied the chloride concentration on the inside (cytoplasm) or outside (medium) of intact erythrocytes. Internal concentrations were altered by treating the cells with nystatin. With 600 mM Cl^- inside, variations of extracellular Cl^- from 150 mM to 600 mM had no significant effect on the rate of ^{36}Cl exchange at 0°C , regardless of whether external Cl^- was replaced by sucrose, sucrose-citrate, or gluconate. In contrast, when external Cl^- was kept constant (with sucrose added to balance the osmolarity), an increase in internal Cl^- concentration from 150 mM to 600 mM caused a 40 ± 3 percent (SEM, $n=6$) inhibition of Cl^- exchange. This was not significantly different from the 43 ± 3 percent ($n=6$) inhibition which resulted when both internal and external Cl^- were raised from 150 mM to 600 mM. Similar results were obtained when gluconate or citrate-sucrose was used to balance the external osmolarity. Thus, the inhibitory effect of Cl^- is primarily exerted at the inside of the cell, indicating that the Cl^- modifier site faces the cytoplasm. This result further implies that the Cl^- modifier site is different from the external site at which N-(4-azido-2-nitrophenyl)-2-aminoethyl sulfonate (NAP-taurine) inhibits Cl^- exchange, despite the fact that both sites have similar Cl^- affinities. (Supported by NIH Grant AM 27495).

M-AM-E2 PHOSPHATE-CHLORIDE EXCHANGE IN HUMAN RED BLOOD CELLS: MONOVALENT vs. DIVALENT PHOSPHATE TRANSPORT. K. R. Runyon and R. B. Gunn. Physiology Dept., Emory University, Atlanta, GA 30322.

Initial 32-phosphate influx was measured into normal human red cells containing 110 mM Cl^- , $\text{pH}_{\text{in}} = 7.6$ at 20°C as a function of external pH and total external phosphate. Gluconate was used as the spectator anion and dinitrostilbene-disulfonate inhibited more than 95% of the influx. At pH_0 values between 6.45 and 8.0, where the chloride exchange flux is independent of pH_0 , the phosphate flux was a single Michaelis-Menten function of monovalent phosphate concentration (H_2PO_4^-). $V_{\text{max}} = 37 \pm 3$ mmol/(kg cell solids \cdot min); $K_{\text{P}04}^{\text{out}} = 147 \pm 13$ mM. If divalent or undissociated phosphoric acid was considered as substrate, the flux was complexly related to both concentration and pH_0 . At pH_0 values below pH 6.45, the H_2PO_4^- flux was inhibited as is chloride flux with a $\text{pK} \sim 5.3$. At very low pH_0 (4.4-4.6), the flux was a sigmoid function of H_2PO_4^- which can be modeled by assuming that ($\text{H}^+ + \text{H}_2\text{PO}_4^-$) is also transported but at a slower rate, in analogy with the slower transport of ($\text{H}^+ + \text{Cl}^-$) compared with Cl^- transport (Jennings, M., J. Mem. Biol. 40:365, 1978). Phosphate influx was competitively inhibited by Cl^- with $K_i^{\text{Cl}} = 2.7$ mM. These data together with previous observations (Gunn, R. et al., Fed. Proc. 39:1715, 1980 abstr.) that only monovalent phosphate appears to inhibit chloride exchange at 0°C demonstrate that the anion transporter treats phosphate as only a monovalent anion like chloride (except that K_s is larger and V_{max} is smaller) and differently from sulfate, whose influx is activated by H^+ (Mifanick, M. and R. Gunn, Am. J. Physiol., in press). The activating effect of protons is due to the production of monovalent substrate and the inhibiting effect of protons is due to the titration of the same group that inhibits chloride transport but activates sulfate-proton co-transport. (Supported by NIH grant HL 28674).

M-AM-E3 THE EFFECT OF METABOLIC DEPLETION ON THE MODES OF OPERATION OF THE FUROSEMIDE-SENSITIVE Na^+ , K^+ - Cl^- CO-TRANSPORT IN HUMAN ERYTHROCYTES. G. DAGHER*, C. BRUGNARA, M. CANESSA (intr. by R.P. GARAY). *INSERM U7, NECKER Hospital, Paris, FRANCE, Dept of Physiology, Harvard Medical School, Boston, MA. 02115.

Red blood cells from 3 subjects were metabolically depleted by either starvation (12 hrs) or iodoacetamide + inosine treatment (2 hrs). Cation content was then modified with nystatin. ATP depletion (70 moles/l.cell) induced (i) a decrease (60 ± 22 %) in the maximal velocity of the furosemide-sensitive (F-S) Na^+ and K^+ efflux into choline or Na^+ media without alteration of the affinity for internal Na^+ , (ii) a decrease (70 ± 21 %) in the F-S Na^+ and K^+ influx (Na_0 125, K_0 20 mM) into cells containing 20 mmole/l.cell of Na_i . Thus the net Na^+ efflux and the net K^+ efflux were reduced by 65 ± 25 %. The K_0 -stimulated Na^+ influx and the Na_0 -stimulated K^+ influx was reduced by 65 ± 25 % after ATP depletion.

The trans-inhibition of the F-S Na^+ efflux by Na_0 and K_0 and the cis-stimulation of the K^+ efflux by Na_i is similar in percentage in control and metabolically depleted cells.

These results suggest that metabolic depletion reduced the turnover rate of the Na^+ , K^+ -co-transport system.

M-AM-E4 PCMBS REVERSIBLY STIMULATES CHLORIDE-DEPENDENT Na AND K EFFLUXES IN HUMAN RED CELLS. W.F. Schmidt, R. Breslow, and M. Haas, Departments of Physiology, Pediatrics, and Pathology, Yale University School of Medicine, New Haven, CT 06510.

P-chloromercuribenzenesulfonic acid (PCMBS) reversibly increases Na and K fluxes across the human red cell membrane (Sutherland et al., *J Cell Physiol* 69:185, 1967). We report here that a large fraction of these PCMBS-induced fluxes has a specific anion requirement for Cl or Br. Cells were loaded to contain either Cl, Br, methyl sulfate, or NO₃ as the major intracellular anion, and tracer effluxes of Na (²²Na) and K (⁸⁶Rb) were measured for 20 min at 37° C into tetramethylammonium (TMA) media containing the same anion that was present intracellularly. Addition of 1 mM PCMBS caused a 10-20 fold increase in K efflux and a 5-10 fold increase in Na efflux in Cl or Br cells, but only slight increases in efflux in cells containing NO₃ or methyl sulfate. Anion substitution had no apparent effect on PCMBS binding. The stimulatory effect of PCMBS was partially reversed (30-40%) by simply washing the cells. More complete reversal was obtained by brief exposure of PCMBS-treated cells to compounds containing free -SH groups. Cells preincubated 15 min with 1 mM PCMBS, then washed and resuspended in media containing 1 mM dithiothreitol, exhibited Na and K effluxes only slightly higher than those in control cells never exposed to PCMBS. Cysteine (2 mM) was less effective. Replacing TMA with K, Li, or choline had little effect on PCMBS-stimulated cation effluxes. Small but reproducible decreases in Na and K effluxes were observed when TMA was replaced by Na. Furosemide (1 mM) did not alter PCMBS-stimulated effluxes, but appeared to interfere with PCMBS binding to the membrane. (Supported by Am. Heart Assoc., Conn. affiliate, Grant #11-207-823)

M-AM-E5 IMMUNOLOGICAL IDENTITY OF K⁺/Cl⁻ COTRANSPORT IN LOW K⁺ SHEEP RED CELLS STIMULATED BY CELL SWELLING OR N-ETHYLMALDEIMIDE. P.K. Lauf, Dept. Physiology, Duke Univ. Med. Center, Durham, N.C. 27710.

Ouabain-insensitive K⁺/Cl⁻ cotransport in low K⁺ (LK) sheep red cells is stimulated by either cell swelling in hyposmotic media (Dunham & Ellory, *J. Physiol.* 318, 1981, 511), or by N-ethylmaleimide (NEM) in isosmotic solutions (Lauf, *J. Memb. Biol.* 73:1983, 237). In K⁺(Rb⁺) media this K⁺/Cl⁻ flux is furosemide sensitive (FS) (Lauf, *J. Memb. Biol.* 77:1984, 247). Although the fractional stimulation of K⁺/Cl⁻ flux by NEM is the same at any given cell volume, the operational identity of the fluxes elicited by the two stimuli is still controversial, particularly since the NEM stimulated K⁺/Cl⁻ flux is metabolically dependent (Lauf, *Am. J. Physiol.* 245, C14, 1983, 44). Immunological studies with anti-L₁ antibody which reduces K⁺ fluxes by both stimuli should clarify further the functional and structural relationship between the two flux activities. I have studied the effect of anti-L₁ on FS K⁺/Cl⁻ fluxes in LK cells stimulated by swelling or NEM. Incubation of NEM treated or swollen (250 mOsm) LK red cells each with 5 different charges of L₁ antisera lead to 51 ± 7 or 52 ± 6 (SEM) % inhibition of K⁺/Cl⁻ flux induced by either stimulus. Furthermore, the fractional inhibition of the FS K⁺/Cl⁻ fluxes stimulated by both NEM or cell swelling was identical at all anti-L₁ concentrations tested, and saturated only at highest antiserum concentrations consistent with low binding affinities reported by us (Lauf & Sun, *J. Memb. Biol.* 28:1976, 351). When anti-L₁ was absorbed with NEM treated or control LK cells, its ability to reduce FS K⁺/Cl⁻ in either NEM treated or swollen LK cells was lost. Hence 1. NEM does not destroy the L₁ antigen, 2. the L₁ antigenic site is different from the site of NEM reaction, and 3. K⁺/Cl⁻ cotransport elicited by both stimuli may be carried out by molecules which are immunologically identical or by one and the same transporter. Supported by PHS AM 28.236.

M-AM-E6 USE OF A FLUORESCENT PROBE TO MONITOR THE TIME COURSE OF RED CELL MEMBRANE POTENTIAL AFTER OSMOTIC SHOCK. John D. Bisognano and James A. Dix, Department of Chemistry, State University of New York, Binghamton, NY 13901.

The fluorescence of the probe, 3,3'-dipropylthiadicarbocyanine (di-S-C₃(5)), is sensitive to membrane potential in human red cells. We have used di-S-C₃(5) to monitor the time course of membrane potential upon cell shrinkage. Cells shrunk with sucrose exhibit an initial rapid rise in probe fluorescence (within the time resolution of the dye, about 30 sec); the rise is followed by a slow (8 min) decrease in fluorescence. If cells are shrunk with KCl or NaCl, however, the fluorescence initially decreases slightly, then remains constant for 30 minutes. Treatment of the cells with the anion transport inhibitor, 4,4'-diisothiocyano-2,2'-disulfonic stilbene (DIDS), or the sodium transport inhibitor, amiloride, does not affect the time course. Treatment of the cells with the potassium carrier, valinomycin, abolishes both the initial and the slow time course seen with the sucrose shrink. Control experiments indicate that ionic strength, scattering, pH, or mixing artifacts are not important. The amplitude of the initial change in fluorescence seen upon cell shrinkage is in qualitative agreement with the Stewart-Jacobs model of the red cell; the slow time course seen with the sucrose shrink may represent a voltage-dependent cation efflux from the red cell. Supported by NIH grant HL29488.

M-AM-E7 TEMPERATURE, OSMOTIC FRAGILITY, AND RED CELL MEMBRANE PHENOMENA.

Gary V. Richieri and Howard C. Mel, Department of Biophysics and Medical Physics, Donner Lab, University of California, Berkeley CA 94720

Temperature has long been known to be a major determinant of red cell fragility: the higher the temperature the greater the resistance to osmotic hemolysis. Explanations offered for this phenomenon have included: (1) an increase in membrane surface area with temperature; (2) a decrease in isotonic volume with temperature; and (3) a temperature-dependent increase in potassium leakage at the cell's critical volume. Using several techniques of resistive pulse spectroscopy (Akeson and Mel, *Biochim. Biophys. Acta* 718: 201 (1982)) we have investigated osmotic fragility and the interrelated properties of volume, form, and surface area for intact cells, hemolysing cells and ghosts. New results are reported on the temperature dependence of surface area, isotonic volume, and critical volume. From these results we arrive at a unifying view of these several factors insofar as they effect osmotic fragility. Properties of the cytoskeleton play a key role in this view. One noteworthy conclusion from this work is that under transient conditions the red cell membrane can stretch by more than 14% without hemolysing. Another is that in the steady state, the membranes of electrically impermeable resealed ghosts can remain extended by more than 10%, compared with membranes of the corresponding unhemolysed/intact red cells.

M-AM-E8 REVERSIBLE AND IRREVERSIBLE MODIFICATION OF MEMBRANE PERMEABILITY BY HIGH INTENSITY ELECTRIC PULSES. Engin H. Serpersu and Tian Yow Tsong, Department of Physiological Chemistry, The Johns Hopkins University School of Medicine, Baltimore, Maryland 21205

Electric field of kV/cm and of microsecond duration is known to perforate cell membranes (see e.g. Tsong, *Bioscience Reports*, 3, 487 (1983)). However, kinetics of the electric breakdown and the reversibility of pores thus formed remain unclear. To answer these questions we have exposed erythrocytes, in an isotonic saline, to a 3.7 to 4.2 kV/cm electric pulse of duration 0.3 to 20 microseconds. Changes in the membrane permeability was monitored by the uptake, above a controlled sample, of the Rb tracer. The pulse width required to perforate erythrocyte membrane using a 3.7 kV/cm field strength was less than 1 microsecond, consistent with an earlier measurement of the time dependent membrane conductance induced by the electric field. After the initial membrane perforation there was a rapid reformation of the permeation barrier to sucrose tracer. However, at 4°C the membranes remained leaky to Rb ion overnight, and the red cells eventually lysed due to the colloid osmotic swelling. The electric field perforated membranes could be resealed by a proper procedure (Kinosita & Tsong, *Nature* 268, 438 (1977)), and kinetics of the resealing at 37°C was followed by the return of the permeation barrier to Rb ion. By this method we have shown that pores large enough to admit sucrose tracer could be completely resealed without loss of the hemoglobin contents. The experiment indicates that electric breakdown of red cell membranes is an irreversible process. However, resealing can be achieved in an osmotically balanced medium, at 37°C. The resealed membranes are indistinguishable from the untreated membrane with respect to their permeability to the Rb ion. (Supported by NIH Grant GM 28795).

M-AM-E9 FLUORESCENCE MEASUREMENTS IN SCATTERING AND ABSORBING CELL SUSPENSIONS (e.g. RBC)

Josef Eisinger and Jorge Flores, AT&T Bell Laboratories, Murray Hill, NJ 07974

We have devised a semi-empirical method for measuring fluorescence yield and polarisation in strongly scattering and absorbing samples and have tested it in suspensions of red blood cells (RBC) and ghosts at hematocrits up to 10^{-3} . If h is the cell titre, ϕ is the probe's quantum yield and n the number of fluorescent probes per cell, the fluorescence is proportional to $nh\phi$ and is attenuated in the sample according to a wavelength-dependent extinction coefficient $\alpha(\lambda)$, which accounts for both absorption and scattering losses. The observed fluorescence intensity I is therefore proportional to $nh\phi \exp[-\alpha(\lambda)h]$, so that a plot of $\ln(I/h)$ vs h is a straight line with slope $\alpha(\lambda)$ and an intercept proportional to $\ln n\phi$. By measuring the fluorescence of different cells, at a series of titres, their relative yields may therefore be determined. We have tested this technique by measuring ϕ of 1-pyrenehexadecanoic acid (PHD) in the membranes of intact RBC and ghosts at the pyrene monomer and excimer wavelengths (377 and 479 nm). The excimer/monomer yield ratio, which reflects the lateral mobility of PHD was (1.15 ± 0.1) times greater in RBC than in ghosts. This was confirmed by employing a set of paired samples of 1:1 mixtures of cells and their ghosts, with the probes in the membrane of RBC in one case and that of the ghost, in the other. With scattering and absorption the same in these sample pairs, so were the slopes $\alpha(377 \text{ nm})$. The same was true at $\lambda=479 \text{ nm}$, but $\alpha(479)=0.55\alpha(377)$ because there is less absorption and scattering at the longer wavelength. A similar approach permits the determination of the fluorescence polarisation of membrane probes in intact RBC. By its use, the rotational relaxation of probes in the membranes of different RBC and in ghosts was compared. Finally, the activation energy for lateral diffusion of PHD in the membranes of RBC and ghosts was measured to be 3.53 ± 0.1 and $3.49 \pm 0.1 \text{ kcal M}^{-1}$, respectively.

M-AM-E10 BLOOD PLATELET AGGREGOMETRY -- THE PROPOSED USE OF SCATTERED INSTEAD OF TRANSMITTED LIGHT. Paul Latimer, Department of Physics, Auburn University, AL 36849.

The aggregation of blood platelets suspended in plasma (prp) is usually observed with a conventional transmittance photometer. Aggregation is indicated by an increase in transmittance. Recently we proposed methods based on conventional light scattering theory to predict how aggregation should influence observable light (P. Latimer (1983), Appl. Opt. 22, 1136). Now new evidence is offered of the validity of the assumptions on which the methods are based. These theoretical methods confirm most previous interpretations of aggregometer results based on empirical evidence. However, it was found that the results should be sensitive to the optical design of the transmittance photometer. Now we find from light scattering theory that an aggregometer which observes light scattered at small angles ($1-4^\circ$) should be 10 or more times as sensitive as one based on transmittance. The small angle scattered signal is predicted to increase much more rapidly with aggregation than does the transmitted signal. Experimental evidence obtained with aggregates of latex spheres is presented to support these predictions.

M-AM-E11 REGULATION OF THE PENTOSE PHOSPHATE PATHWAY IN THE HUMAN ERYTHROCYTE. V. DeBari and A. Bennun; The Renal Laboratory, St. Joseph's Hosp. & Med. Ctr., Paterson, NJ and Dept. of Zoology, Rutgers University, Newark, NJ.

Erythrocytes in conditions which show little or no guanylate or adenylate cyclase activity, take up cyclic nucleotides from blood. Studies were done independent of time-requiring uptake, by incubating human erythrocytes in isotonic medium with the dibutyl derivatives of cAMP and cGMP and in a hypotonic medium which rendered the cell membrane "leaky," therefore time-independent permeable to cAMP and cGMP. At cAMP and cGMP concentrations of 0.1mM and above, the amount of $^{14}\text{CO}_2$ generated from $1-^{14}\text{C}$ -glucose was decreased significantly. This effect was suppressed by 4.6mM theophylline. Inosine and ribose, which are catabolites of cAMP and cGMP also decreased formation of $^{14}\text{CO}_2$ from $1-^{14}\text{C}$ -glucose. Accordingly, it is postulated that in the absence of theophylline, the activity of phosphodiesterase resulted in AMP and GMP formation. These mononucleotides enter into the purine salvage cycles to form cold ribose phosphate. Hence, conditions under which much more ribose-5-phosphate than NADPH is required could allow for the observed decrease in the rate of utilization of $1-^{14}\text{C}$ -glucose by the oxidative branch of the HMP pathway. This would explain that the magnitude of the inhibition of $^{14}\text{CO}_2$ release by cyclic nucleotides was greater than the one expected from cold ribose phosphate diluting the label of the pool of intermediates generated from $1-^{14}\text{C}$ -glucose. Accordingly, metabolism of cyclic nucleotides prevents diffusion equilibria allowing the erythrocyte's continuous uptake of cyclic nucleotides and providing therefore a detoxication mechanism that could compensate for renal failure.

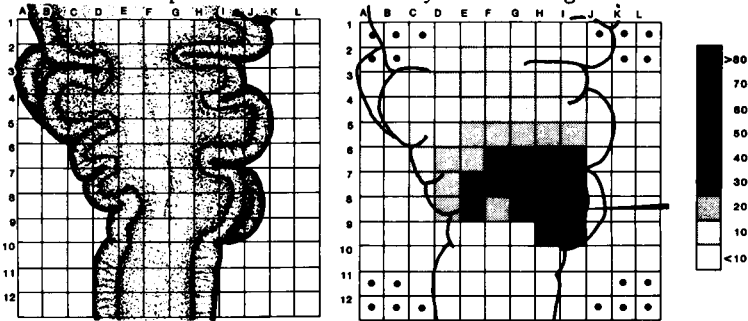
M-AM-E12 EFFECT OF ETHANOL ON THE FLUIDITY OF ERYTHROCYTE GHOST MEMBRANES. Preeti Gangola and Harish C. Pant. Laboratory of Preclinical Studies, National Institute on Alcohol Abuse and Alcoholism, 12501 Washington Avenue, Rockville, Md. 20852

The fluorescence polarization of hydrophobic probe 1,6-Diphenyl-1,3,5-hexatriene (DPH) was used to study the effect of ethanol on the fluidity of erythrocyte ghost membranes. We measured the fluorescence intensity, polarization, anisotropy and lifetime of DPH incorporated into the membranes. The rotational rate of the probe was estimated using the Perrin's equation. The erythrocyte ghost membranes were prepared from rat blood by the method of Hanahan and Ekholm (1974) (Methods in Enzymology 31, 168-172). The membrane suspension was diluted in 130 mM NaCl + 20 mM Tris (pH 7.4) to a final concentration of 300 μg protein/ml, and the DPH concentration used was 10 μM . Ethanol was added to the membrane suspension in the concentration range 0-450 mM. The measurements were performed at 25°C . Addition of ethanol to the membranes decreased the polarization of DPH in a nonlinear fashion. A monotonic decrease was observed up to 100 mM of ethanol whereas no significant change was noticed between 120-200 mM, and higher ethanol concentrations further decreased the polarization. The polarization value in the presence of 450 mM ethanol is 0.342 as compared to 0.361 in its absence. Increase in ethanol concentration also decreased the fluorescence intensity and lifetime. The calculated rotational rate showed an increase with increasing concentrations of ethanol, suggesting that the environment of the probe becomes more fluid by the addition of ethanol to the membranes. In other words, ethanol decreases the microviscosity of erythrocyte ghost membranes.

M-AM-F1 ANISOTROPIC POLARIZATION SPREAD IN AN EXOCRINE GLAND: 2-DIMENSIONAL IMAGING USING MSORTV

D.M.SENSEMAN*, I.S.HORWITZ**, B.M.SALZBERG**. U of Texas at San Antonio* and U of Pennsylvania**

The technique of MULTIPLE SITE OPTICAL RECORDING OF TRANSMEMBRANE VOLTAGE (MSORTV) was used to investigate regional spread of hyperpolarizing current injected into the salivary gland of the snail *Helisoma trivolvis* with an intracellular microelectrode. By projecting a real image of the gland stained with NK2367 on to a 12 X 12 photodiode array, changes in membrane potential produced by the current injection could be monitored simultaneously in up to 124 contiguous gland regions. Results obtained in a typical experiment are shown below. Drawing at left shows gland regions monitored by each array element. A graphic image of polarization spread was obtained by converting normalized optical signals into grey-scale values and presenting these on an outline of the preparation. For the particular experiment shown at right, the percentage change in membrane potential produced by a 20 na, 500 ms current pulse is represented with a 9-level grey scale. As can be seen, the spread of polarization is anisotropic being greater along the lateral than the longitudinal gland axis. Supported by USPH grants DE-05271 and NS-16824.

**M-AM-F2 EFFECTS OF GENERAL AND LOCAL ANESTHETICS ON INTERCELLULAR COUPLING IN THE HEART MUSCLE**

Jacek A. Wojtczak (Intr. by Paul F. Cranefield), Medical Center of Postgraduate Education, Warsaw and Rockefeller University, New York 10021.

Effects of local anesthetics (lidocaine, trifluoperazine) on mechanical tension and intercellular electrical coupling approximated as changes of internal longitudinal resistance (r_i) were tested in normal and calcium overloaded feline papillary muscles. Oil-gap method (Wojtczak, Circ. Res. 44,88,1979) was used to measure r_i . Calcium overloading was induced by superfusion with 400% hypertonic solution. Contracture (increase in resting tension) and increase in r_i induced by this superfusion could be reduced by withdrawal of extracellular calcium or addition of $10^{-4}M$ trifluoperazine (TFP). Preventive action of lidocaine ($10^{-4}M$) was much less marked. TFP and lidocaine did not change r_i in normal preparations.

Effects of general anesthetics (halothane, aliphatic alcohols) on r_i were tested using modified sucrose-gap method (Kleber, Pflugers Arch. 345,195,1973). Halothane (2-3%) and medium-chain length alcohols (1-5mM hexanol, heptanol and octanol) produced fast and reversible intercellular uncoupling. TFP ($10^{-4}M$) was unable to prevent uncoupling produced by halothane and alcohols which suggests that mechanism of intercellular uncoupling produced by these drugs may be different from the one during calcium overloading. TFP acts also as calmodulin inhibitor which implies that calmodulin may be involved in calcium-induced uncoupling and that inhibition of calmodulin action may prevent this type of uncoupling.

M-AM-F3 CYTOPLASMIC SURFACE AND INTRAMEMBRANE COMPONENTS OF RAT HEART GAP JUNCTIONAL PROTEIN.

Chellakere K. Manjunath and Ernest Page, The University of Chicago.

Gap junctions (GJ) purified from rat hearts in the presence or absence of proteolysis inhibitors by a modification of our published method (Biochem. J. 205: 189-194, 1982), were examined by sodium dodecylsulfate polyacrylamide gel electrophoresis (SDS-PAGE) and by electron microscopy (EM) of glutaraldehyde- and OsO_4 -fixed, uranium- and lead-stained thin-sectioned pellets. In absence of proteolysis inhibitors, SDS-PAGE yielded a single major protein band at M_r 29,500, and EM of the GJ showed that their cytoplasmic surfaces were smooth. SDS-PAGE of GJ prepared with phenylmethylsulfonyl fluoride (PMSF) showed appearance of a broad new major protein band at M_r 44,000-47,000 and markedly reduced intensity of the M_r 29,500 protein band. EM of GJ prepared with PMSF revealed presence of a fuzzy layer on their cytoplasmic surfaces. 8 M urea and 0.3% deoxycholate and 0.3% N-lauryl sarcosine do not dissociate the 44,000-47,000 band protein and do not remove the fuzzy cytoplasmic surface layer. With other proteolysis inhibitors (EDTA, leupeptin), the SDS-PAGE pattern does not change from that in absence of such inhibitors, and the GJ thus isolated have smooth cytoplasmic surfaces. In intact rat left ventricles fixed by coronary vascular perfusion with isosmolar OsO_4 -Na cacodylate (pH 7.3) (or glutaraldehyde-cacodylate followed by OsO_4), cytoplasmic surfaces of GJ between myocytes always have a fuzzy layer. We conclude that rat heart GJ protein consists of an intramembrane component (M_r 29,500) and a cytoplasmic surface component (M_r 14,500-17,500) which corresponds to the fuzzy layer and is cleaved by a PMSF-inhibitable endoprotease. Supported by USPHS Grants HL 20592 and 10503.

M-AM-F4 FERTILIZATION-INDUCED CHLORIDE AND POTASSIUM CONDUCTANCES IN EGGS OF THE FROG, *RANA* *PIPIENS*. Lyanne C. Schlichter and Laurinda A. Jaffe (Physiology Dept., Univ. of Connecticut Health Center, Farmington, CT 06032).

Fertilization of the frog egg elicits a membrane depolarization that lasts 10-20 min and is caused in part by the opening of Cl channels (Cross and Elinson, 1980, *Dev. Biol.* 75: 187-198). We used the voltage-clamp technique to measure ion conductances (g) during fertilization. Before fertilization, a voltage-sensitive g_{Na} is present (Schlichter, 1983, *Dev. Biol.* 98: 47-59, 60-69). On fertilization, two new conductances (g_K and g_{Cl}) appear, reach a maximum in 1-2 min, then decrease more slowly. After fertilization g_{Na} disappears. g_K and g_{Cl} were separated by blocking g_K with external tetraethylammonium. g_{Cl} is voltage dependent, increasing above about 0 mV. The same conductance changes are elicited by monospermy or by polyspermy or by artificial activation.

At fertilization, the surface area of the egg, determined by capacitance measurements, increases 2-fold, because of cortical vesicle exocytosis; surface area subsequently decreases. To examine whether this addition and subtraction of membrane might account for the sequential changes in membrane conductance, we compared the kinetics of the capacitance and conductance changes. Membrane conductance increases more rapidly and subsequently decreases more rapidly than does capacitance. We conclude that the addition and subtraction of membrane is not the major factor in the regulation of conductance at fertilization. The decrease in surface area could be a mechanism for the decrease in g_{Na} . Supported by an NSERC postdoctoral fellowship to Lyanne C. Schlichter and NIH grant HD14939 to Laurinda A. Jaffe.

M-AM-F5 A SOLUBLE FRACTION OF SPERM TRIGGERS CORTICAL GRANULE EXOCYTOSIS IN SEA URCHIN EGGS. Gerald Ehrenstein⁺⁺, Brian Dale⁺⁺, and Louis J. DeFelice^{##}, ^{*}NINCDS, NIH, Bethesda, MD 20205, [#]Dept. of Anatomy, Emory University, Atlanta, GA 30322, and ^{*}Marine Biological Laboratory, Woods Hole, MA 02543.

One of the first events in the activation of sea urchin eggs is the exocytosis of cortical granules leading to the formation of the fertilization membrane. Although it has been well established that an increased concentration of intracellular calcium is necessary for this event, the question remains as to how the spermatozoon triggers the calcium increase.

Our experiments on sea urchin gametes indicate that:

- 1) injection by pressure into unfertilized eggs of a small volume (less than 0.1% of egg volume) of a soluble spermatozoa fraction that is isosmotic with seawater causes formation of the fertilization membrane.
- 2) injection by pressure into unfertilized eggs of a small volume (less than 0.1% of egg volume) of distilled water causes formation of the fertilization membrane.
- 3) the active component in the soluble sperm fraction is not free calcium.

We suggest that the egg contains internal stores of both calcium and a calcium-channel agonist, and that the spermatozoon triggers the cortical reaction by introducing into the egg a component that causes the release of the calcium-channel agonist into the cytoplasm. This agonist opens calcium channels, releasing calcium into the cytoplasm and causing local cortical granule exocytosis. The agonist also causes the release of more agonist, opening more calcium channels and resulting in a propagation of exocytosis.

M-AM-F6 A23187 AND CALMODULIN ANTAGONISTS INHIBIT METABOLIC COUPLING BETWEEN PARTURIENT RAT MYOMETRIAL SMOOTH MUSCLE CELLS. Cole, W.C. & R.E. Garfield, Department of Neuroscience, McMaster University, Hamilton, Ontario, Canada, L8N.

Parturition in rats is marked by a concomitant increase in the area of gap junctions (GJ's) and metabolic coupling between myometrial smooth muscle cells (Cole *et al.*, *Biophys. J.* 41: 84a). We have tested the hypothesis that the permeability of these junctions is modulated by the level of cytoplasmic free Ca^{++} and the Ca^{++} -dependant regulatory protein calmodulin, by studying the effects of the ionophore A23187 and calmodulin antagonists, chlorpromazine, fluphenazine and calmidazolium on metabolic coupling in the parturient myometrium. One portion of strips of longitudinal myometrium was exposed to ³H-2-deoxyglucose (2DG) and the distribution of tracer in the strips determined after a five hour period for diffusion in the presence or absence of drug added to the bathing media. Tracer diffusion in the extracellular space was studied using ³H-sucrose. The distribution of 2DG in strips exposed to A23187 was equivalent to that of sucrose, hence, little or no intracellular diffusion of tracer through the strip occurred in the presence of elevated cytoplasmic free Ca^{++} . The calmodulin antagonists were found to reduce the longitudinal distribution and diffusion coefficient (D in $cm^2 \cdot sec^{-1}$) of 2DG in treated compared to control strips (chlor. $D = 0.47 \times 10^{-6}$; flu. $D = 0.57 \times 10^{-6}$; calmid. $D = 0.52 \times 10^{-6}$; control $D = 2.26 \times 10^{-6}$), hence, calmodulin appears to regulate GJ channel permeability. These data are consistent with the hypothesis that metabolic coupling in the parturient myometrium may be modulated by Ca^{++} and calmodulin. Supported by MRC of Canada, a Canadian Heart Foundation Studentship to W.C.C., and an Ontario Heart Foundation Fellowship to R.E.G.

M-AM-F7 THEORETICAL MODELS OF CELL ADHESION, George I. Bell and Micah Dembo, Theoretical Division, Los Alamos National Laboratory, Los Alamos, New Mexico 87545

Recent theoretical calculations and experimental evidence suggest that there is a strong nonspecific repulsive force between most cells, arising from electrostatic forces and from solvent exclusion from the hydrated polymers extending from their surfaces (steric stabilization). We have developed theoretical models for the competition between such repulsion and bonding mediated by specific receptors or receptor ligand complexes between the cells. Assuming that "receptors" on at least one of the cells are mobile we have computed the equilibrium (minimum free energy) configurations, obtaining contact area, number of intercellular bonds and cell-cell (or cell-substrate) separation distances as functions of the cell areas, number of receptors, bond equilibrium constants and parameters characterizing the repulsion. Parameters have been estimated and results will be compared with experiment. Several model variations have been treated depending on whether receptors on the second cell or surface are mobile or fixed, whether or not the molecules responsible for the repulsion may diffuse out of the contact area, etc. and results of several models will be compared.

M-AM-F8 ACTION POTENTIALS ELICITED BY ARTERIAL PRESSURE PULSATIONS IN CANINE SINUS NODE.

W.T. Woods, Jr., Department of Physiology and Biophysics, University of Alabama in Birmingham, University Station, Birmingham, AL 35294

The sinus node (SN) in the isolated canine right atrium requires perfusion through its central artery (SNA) to maintain spontaneous generation of pacemaker impulses. Physiologic solution was perfused into the SNA's of 12 isolated canine right atria under pulsatile or non-pulsatile pressure to determine how pressure pulsations affect action potentials recorded with micro-electrodes in pacemaker cells. Each excised right atrium was placed immediately into an organ bath at 37°C and a catheter was inserted into its SNA. Unperfused atria became quiescent within 30 min.; then SNA perfusion was begun. Under non-pulsatile pressure (100 mm Hg) SN cells began to fire at slow rates (12 ± 5 impulses per min.) and gradually increased, finally stabilizing at 103 ± 20 impulses per min. However, under pulsatile pressure (140/60 mm Hg, 70 pulses/min.) SN cells generated one action potential for each pressure pulsation as soon as perfusion began. When the rate of pulsation was increased to 90 pulses/min., the rate of SN cell firing increased to a stable 90 impulses/min. within 10 min. SN action potentials were always preceded by SNA pulsations and were always followed by atrial working cell action potentials. After 75 ± 15 min., amplitude of the SNA pulsations had to be increased to 190/40 mm Hg to elicit SN action potentials. After 105 ± 15 min. SNA pulsations no longer elicited SN action potentials. Thus, for at least 2 hrs. after isolation of the canine right atrium, a coupling exists between oscillating SNA pressure and oscillating SN action potentials. Further studies will determine the cellular basis for this mechano-electrical coupling.